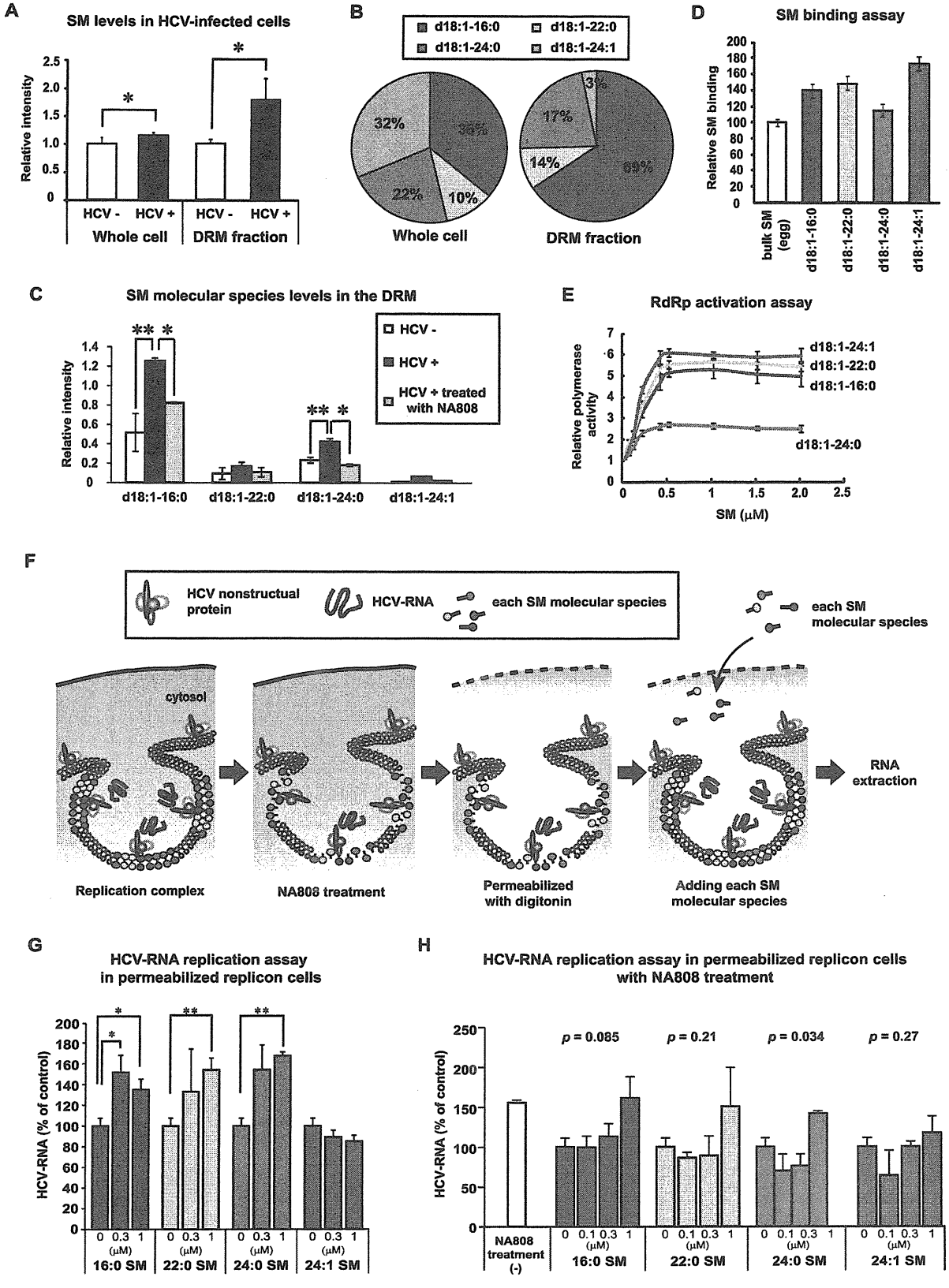
A
SM levels in HCV-infected cells
Relative intensity
HCV - HCV + HCV - HCV +
Whole cell
DRM fraction
B
d18:1-16:0
d18:1-22:0
d18:1-24:0
d18:1-24:1
32%
22%
10%
17%
14%
3%
Whole cell
DRM fraction
D
SM binding assay
Relative SM binding
bulk SM (egg)
d18:1-16:0
d18:1-22:0
d18:1-24:0
d18:1-24:1
C
SM molecular species levels in the DRM
Relative intensity
HCV -
HCV +
HCV + treated with NA808
d18:1-16:0
d18:1-22:0
d18:1-24:0
d18:1-24:1
E
RdRp activation assay
Relative polymerase activity
SM (μM)
d18:1-24:1
d18:1-22:0
d18:1-16:0
d18:1-24:0
F
HCV nonstructual protein
HCV-RNA
each SM molecular species
each SM molecular species
cytosol
RNA extraction
Replication complex
NA808 treatment
Permeabilized with digitonin
Adding each SM molecular species
G
HCV-RNA replication assay in permeabilized replicon cells
HCV-RNA (% of control)
(μM)
16:0 SM
22:0 SM
24:0 SM
24:1 SM
H
HCV-RNA replication assay in permeabilized replicon cells with NA808 treatment
p = 0.085
p = 0.21
p = 0.034
p = 0.27
HCV-RNA (% of control)
NA808 treatment (-)
(μM)
16:0 SM
22:0 SM
24:0 SM
24:1 SM

Figure 6. Specific sphingomyelin molecular species upregulated by HCV promote HCV replication on the detergent-resistant membrane fraction. (**A**) Comparison of the relative amounts of SM, as measured by MS analysis, in whole cells and the DRM fraction of mock-infected (HuH-7 K4 cells) (white, n = 6; whole cells, n = 3; DRM fraction) and HCV (JFH-1)-infected cells (JFH/K4 cells) (black, n = 6; whole cells, n = 3; DRM fraction). (**B**) Composition ratio of SM molecular species in whole cells and DRM fraction of HCV-infected cells. (**C**) Relative intensities of each SM molecular species in the DRM fraction of mock-infected cells (white, n = 2) and HCV-producing cells without (black, n = 2) or with NA808 treatment (gray, n = 2). (**D**) Results of the ELISA SM binding assay (n = 3 each). (**E**) Average activation kinetics of each SM molecular species on HCR6 (genotype 1b) RdRp (n = 3 each). (**F**) Scheme of HCV-RNA replicase assay using digitonin-permeabilized cells. (**G, H**) Effect of each SM molecular species on HCV-RNA in digitonin-permeabilized replicon cells treated without (G) or with 10 nM NA808 (H) (n = 3 each). In all cases, error bars indicate SDs. *$p<0.05$ and **$p<0.01$.
doi:10.1371/journal.ppat.1002860.g006

time course of acute HCV infection in cultured Huh-7.5 cells and observed that specific SM molecular species were decreased 72 h after HCV infection [27]. Given that their study focused on acute HCV infection, the reason for this discrepancy may be due to the severity of infection, suggesting that the influence of HCV infection on sphingolipid metabolism differs between acute and chronic infections. We also demonstrated that HCV infection correlates with increased abundance of specific SM and ceramide molecular species, with the profiles of individual lipids differing for infection by HCG9 (genotype 1a) and HCR24 (genotype 2a). The precise mechanism and meaning of these differences remain to be elucidated.

Our results indicated that SGMS1 expression had a correlation with HCV replication. This indicates that SM synthesized by SGMS1 contributes to HCV replication. A previous report revealed that in cultured cell lines, SGMS1 localizes in Golgi apparatus while SGMS2 localizes in the plasma membrane [28]. Thus, the results of this previous report suggest that SMs synthesized by SGMS1 can be easily incorporated into membranous replication complexes. As for SGMS2, we found that HCV infection significantly increased the expression of SGMS2, although the relationship between SGMS2 and HCV replication was hardly seen in this study. The relationship between SGMS2 and HCV propagation, thus, is an issue that should be elucidated in future studies.

We also demonstrated in this study that reduction of SM molecular species by NA808, a hepatotropic SPT inhibitor with little immunosuppressive activity, inhibits HCV replication in humanized chimeric mice regardless of viral genotype (Figure 4). Notably, treatment with NA808 (5 mg/kg) restored SM and ceramide levels in the liver to the levels observed in uninfected chimeric mice (Figure 5). Apparently, a slight reduction in SM had a significant influence on HCV, indicating that SM plays an important role in the HCV life cycle. SM is required for many viral processes in host-pathogen interactions [29–31]. For instance, viral envelopes of human immunodeficiency virus type 1 (HIV-1) and herpes simplex virus (HSV) are enriched with SM, which is necessary for efficient virus infectivity [32,33]. With regard to HCV, in addition to efficient virus infectivity [34], SM is present in the raft domain, which serves as a site of virus replication, together with other sphingolipids and cholesterol [6]. Moreover, SM is a component of VLDL whose assembly component and pathway is required for HCV morphogenesis and secretion [34,35]. The above-mentioned observations suggest that SM plays a multifaceted role in the HCV life cycle; therefore, SM is likely to be a good therapeutic target.

HCV is thought to replicate in a specialized compartment characterized as a DRM (designated as the membranous replication complex) [6]. SM, cholesterol, and phosphatidylinositol (PI) are thought to be the lipids that make up the membranous replication complex. With regard to PI, several siRNA screening have recently identified type III phosphatidylinositol 4-kinases (PI4K) as crucial host factors for HCV replication [36–39]. In HCV replicon containing cells, PI4P distribution is altered and enriched in the membranous replication complex by PI4KIIIα synthesis. Although the ability of PI to influence membrane bending and regulate intracellular processes (e.g. vesicle fusion, budding, and sorting) has been reported, the role of PI4P in the formation of the membranous replication complex remains to be elucidated. SM and cholesterol organize the solid membrane characterized as the DRM, where HCV replicates [6]. In fact, we and other groups demonstrated that reduction of SM and cholesterol suppressed HCV replication [7,9,12,40]. We performed the immunofluorescent analysis using lysenin. However, lysenin did not co-localize with NS4B protein. To date, it has been reported that lysenin-binding to SM is increased in the form of SM clusters, and that glycosphingolipids hinder lysein-binding to SM [41] Lipid rafts form of HCV replication complex do not have the characters of lysenin-binding to SM.

Further, the role of SM is not only to act as a constituent of the membranous replication complex, but also to bind and activate RdRp [7,8]. In this study, to gain further insight into the HCV membranous replication complex, we attempted to analyze which SM molecular species comprise the membranous replication complex, given that the diversity of molecular species is believed to be responsible for the physiochemical properties of the biomembrane [42] (Figure 6). We found that the composition ratio of SM molecular species observed in this study was quite different between the whole cell and DRM fractions. Further, to identify whether these SM molecular species contribute to HCV replication, we conducted rescue experiments using HCV replicon-containing cells (carrying intact RdRp and active membranous replication complexes) in which each SM molecular species was extrinsically added to replicon cells treated with NA808. However, in this experiment, addition of SM caused cell death. Therefore, we used digitonin-permeabilized semi-intact replicon cells, which enabled us to deliver the extrinsically added SM molecular species directly to the cytosol without catalytic effect and permitted monitoring of intact RdRp and replication complexes. We demonstrated that the specific endogenous SM molecular species (*d*18:1-16:0 and *d*18:1-24:0) enhance HCV-RNA replication, these species being consistent with the two SM molecular species which mainly constitute the DRM. Collectively, these results suggest that the HCV replication complex characterized as DRM is the specialized compartment that is composed of SM molecular species. These findings will provide new insights into the formation of the HCV replication complex and the involvement of host lipids in the HCV life cycle.

Materials and Methods

Ethics statement

This study was carried out in strict accordance with both the Guidelines for Animal Experimentation of the Japanese Association for Laboratory Animal Science and the recommendations in the Guide for the Care and Use of Laboratory Animals of the National Institutes of Health. All protocols were approved by the ethics committee of Tokyo Metropolitan Institute of Medical

Science. The patient with HCV infection who provided the serum samples gave written informed consent before blood collection.

Cells

The HCV subgenomic replicon cells FLR3-1 (genotype 1b, Con-1) was cultured at 37°C in Dulbecco's modified Eagle's medium GlutaMax-I (Invitrogen, Carlsbad, CA, USA) supplemented with 10% fetal bovine serum (FBS) and 0.5 mg/mL G418. HuH-7 K4 cells (cured of HCV by IFN treatment) and the JFH/K4 cells persistently infected with the HCV JFH-1 strain were maintained in DMEM containing 10% FCS and 0.1 mg/mL penicillin and streptomycin sulfate. MH-14 cells were grown in Dulbecco's modified Eagle's medium supplemented with 10% fetal bovine serum, 100 U/mL nonessential amino acids, 0.1 mg/mL penicillin and streptomycin sulfate, and 0.5 mg/mL G418.

siRNA assay

siCONTROL, siSGMS1, and siSGMS2 were purchased from Dharmacon RNA Technologies (Lafayette, CO, USA). The siCONTROL Non-Targeting siRNA #3 was used as the negative control siRNA. We used siRNAs against the HCV genome (siE-R7) [16]. The chemically synthesized siRNAs were transfected into cells using Lipofectamine RNAiMAX (Invitrogen) and Opti-MEM (Invitrogen) by reverse-transfection. Cells were characterized at 96 h after transfection.

Serine palmitoyltransferase activity

We assessed SPT activity in the liver as previously described, with minor modifications [43]. Briefly, frozen cells were homogenized in HEPES buffer (10 mM HEPES, 2 mM sucrose monolaurate, and 0.25 M sucrose, pH 7.4), and homogenates were centrifuged at 10,000×*g* for 20 min. From the resulting supernatant, samples containing 200 μg protein were assayed for SPT activity using [^{14}C]-serine and palmitoyl-CoA (Sigma-Aldrich, St. Louis, MO, USA) as substrates.

Proliferation assay

Human peripheral blood cells (AllCells, Emeryville, CA, USA) were plated onto 96-well plates and treated with phytohemagglutinin with or without immunosuppressant reagents. After 2 days of stimulation, [^{3}H]-thymidine-containing growth medium was added, and the cultures were incubated for another 18 h. T-cell proliferation was assessed by comparing the level of thymidine incorporation to that in the stimulated control.

Anti-hepatitis C virus assay in Huh-7 cells harboring subgenomic replicons

Replication was determined after 72 h with a Bright-Glo luciferase assay kit (Promega, Madison, WI, USA). The viability of replicon cells was determined using a cell counting kit (Dojindo, Kumamoto, Japan) according to the manufacturer's instructions.

Western blot analysis

Cells were resuspended in lysis buffer (10 mM Tris, pH 7.4 containing 1% SDS, 0.5% Nonidet P-40, 150 mM NaCl, 0.5 mM EDTA, and 1 mM dithiothreitol). Ten micrograms of the resulting protein sample were electrophoresed on a 10% sodium dodecyl sulfate-polyacrylamide gel and subsequently transferred to a polyvinylidene difluoride membrane (Immobilon-P; Millipore, Billerica, MA, USA). HCV nonstructural protein 3 (NS3) and nonstructural 5B polymerase (RdRp) were detected with rabbit anti-NS3 polyclonal antibody (R212) and mouse anti-RdRp monoclonal antibody (5B-14) prepared in our laboratory. β-Actin was detected with anti-β-actin monoclonal antibody (Sigma-Aldrich).

Immunofluorescent staining of hepatitis C virus replicon cells

After treatment with 25 nM NA808 for 96 h, FLR3-1 cells were probed with anti-NS3 polyclonal antibody (R212; the primary antibody). Next, an anti-rabbit IgG-Alexa 488 conjugate (Invitrogen) was applied as the secondary antibody.

Thin-layer chromatography analysis

Thin-layer chromatography (TLC) analysis was performed as described previously [9]. Briefly, cells were incubated with [^{14}C]-serine in Opti-MEM (Invitrogen). Cells extracts were obtained using the Bligh & Dyer method [44] and were spotted onto Silica Gel 60 TLC plates (Merck, Darmstadt, Germany) for separation. Radioactive spots were detected using a BAS 2000 system (Fuji Film, Kanagawa, Japan).

Membrane flotation assay

Cells were lysed in TNE buffer (25 mM Tris-HCl, 150 mM NaCl, 1 mM EDTA) and passed 20 times through a 25-gauge needle. Nuclei and unbroken cells were removed by centrifugation at 1,000×*g* for 5 min. After ensuring that the amount of total protein was equivalent across all samples, cell lysates were treated with 1% Triton on ice for 30 min and then subjected to a sucrose gradient (10%, 30%, and 40%). The sucrose gradient was centrifuged at 247,220×*g* in a Beckman SW41 Ti rotor (Beckman Coulter Inc., Brea, CA, USA) for 14 h at 4°C. Fractions (1 mL) were collected from the top of the gradient.

Infection of mice with hepatitis C virus genotypes 1a and 2a

Chimeric mice infected with HCV were prepared as previously described [45]. Briefly, approximately 40 days after the transplantation procedure, mice were intravenously injected with 5×10^5 copies/mouse of HCG9 (genotype 1a) or HCR24 (genotype 2a) that had been collected from patient serum.

Quantification of HCV RNA by real-time polymerase chain reaction

Total RNA was purified from 1 μL of chimeric mouse serum using SepaGene RV-R (Sanko Junyaku Co. Ltd., Tokyo, Japan) and from liver tissue using Isogene (Nippon Gene Co. Ltd., Tokyo, Japan). HCV RNA was quantified by quantitative real-time polymerase chain reaction (PCR) using previously reported techniques [9]. For serum, this technique has a lower limit of detection of 4000 copies/mL. Therefore, samples in which HCV RNA was undetectable were assigned this minimum value.

Quantification of HCV core protein by ELISA

Liver specimens were homogenized in TNE buffer. Aliquots of 5 μg of total protein were assayed for core protein levels with an Ortho HCV core protein ELISA kit (Eiken Chemical, Tokyo, Japan).

Indirect immunofluorescence analysis

The primary antibody for immunofluorescence analysis of liver sections was anti-HCV core protein monoclonal antibody (5E3) [46]. Monoclonal antibody labeling was followed by staining with anti-mouse IgG Alexa-488. The nuclei were stained using 4′,6-diamidino-2-phenylindole (DAPI).

Gene expression analysis

To measure mRNA levels, total RNA samples were extracted from the mouse livers and cDNA was synthesized using a High-Capacity cDNA Reverse Transcription Kit (Applied Biosystems, Foster City, CA, USA). The cDNA solution was assessed by quantitative PCR performed with TaqMan Gene Expression Assays (Applied Biosystems) and an ABI 7700 Sequence Detection System (Applied Biosystems).

Quantification of SM and ceramide in liver

We quantified liver SM and ceramide levels using a mass spectrometer (MS). Electrospray ionization (ESI)-MS analysis was performed using a 4000Q TRAP quadrupole-linear ion trap hybrid MS (AB SCIEX, Foster City, CA, USA) with an UltiMate 3000 nano/cap/micro-liquid chromatography system (Dionex Corporation, Sunnyvale, CA, USA) combined with an HTS PAL autosampler (CTC Analytics AG, Zwingen, Switzerland). The total lipid fractions expected to contain SM and ceramide, were subjected directly to flow injection and were selectively analyzed by neutral loss scanning of 60 Da (HCO_2+CH_3) from SM $[M+HCOO]^-$ in the negative ion mode, and multiple-reaction monitoring using a combination of ceramide $[Cer-H_2O+H]^+$ and the product (long-chain base) $[LCB-H_2O+H]^+$ in the positive ion mode [47,48]. The mobile phase composition was acetonitrile:methanol:water at 6:7:2 (0.1% ammonium formate, pH 6.8) and a flow rate of 10 μL/min. The typical injection volume was 3 μL of total lipids, normalized by protein content.

LC/ESI-MS analysis was performed using quadrupole/time of flight (Q-TOF) micro with an ACQUITY UPLC system (Waters Corporation, Milford, MA, USA) in the negative ion mode and an Agilent 6230 with an Agilent 1290 Infinity LC system (Agilent Technologies, Inc., Loveland, CO, USA) in the positive ion mode. Reversed-phase LC separation was achieved using an ACQUITY UPLC BEH column (150 mm×1.0 mm i.d., Waters Corporation) at 45°C. The mobile phase was acetonitrile:methanol:water at 19:19:2 (0.1% formic acid+0.028% ammonia) (A) and isopropanol (0.1% formic acid+0.028% ammonia) (B), and the composition was produced by mixing these solvents. The gradient consisted of holding A:B at 90:10 for 7.5 min, then linearly converting to A:B at 70:30 for 32.5 min, and then linearly converting to A:B at 40:60 for 50 min. The detailed procedure for LC/ESI-MS was described previously [49,50].

Separation of SM molecular species by HPLC

Bovine milk or brain SM (Avanti Polar Lipids. Inc., Alabaster, AL, USA) was dissolved in chloroform:methanol (2:1), then separated according to molecular species by reversed-phase HPLC. The *d*18:1-16:0, 22:0, and 24:0 molecular species of SM were isolated from bovine milk SM, while the *d*18:1-24:0 and 24:1 molecular species were isolated from brain SM. Bovine milk and brain SM were then separated on Senshu PAK ODS (C18) columns (Senshu Scientific Co., Ltd., Tokyo, Japan) using methanol as the eluting solvent at a flow rate of 1 mL/min. The fatty acid compositions of the purified fractions were analyzed by LC/ESI-MS. The amount of SM in each fraction was quantified using an SM assay kit (Cayman Chemical, Ann Arbor, MI, USA). We confirmed that the purity of each molecular species was approximately 90% without *d*18:1-24:1 (about 70%) (data not shown).

In vitro HCV transcription

In vitro HCV transcription was performed as previously described [8].

SM binding assay using ELISA

An SM binding assay was performed as previously described [8] using rabbit anti-HCV RdRp sera (1:5000) and an HRP-conjugated anti-rabbit IgG antibody (1:5000). Optical density at 450 nm (OD_{450}) was measured on a Spectra Max 190 spectrophotometer (Molecular Devices, Sunnyvale, CA, USA) using the TMB Liquid Substrate System (Sigma).

RNA replication assays in permeabilized replicon cells

The analysis using digitonin-permeabilized replicon cells was performed as previously described [20] with minor modifications. Briefly, MH-14 cells of about 80% confluency were pre-cultured for 2 h in complete Dulbecco's modified Eagle's medium containing 5 μg/mL actinomycin D (Nacalai Tesque, Kyoto, Japan), then washed with cold buffer B (20 mM HEPES-KOH (pH 7.7 at 27°C), 110 mM potassium acetate, 2 mM magnesium acetate, 1 mM EGTA, and 2 mM dithiothreitol). The cells were permeabilized by incubation in buffer B containing 50 μg/mL digitonin for 5 min at 27°C, and the reaction was stopped by washing twice with cold buffer B. The permeabilized cells were then incubated for 4 h at 27°C in the reaction mixture with or without each lipid. The reaction mixture consisted of 2 mM manganese(II) chloride, 1 mg/mL acetylated bovine serum albumin (Nacalai Tesque), 5 mM phosphocreatine (Sigma), 20 units/mL creatine phosphokinase (Sigma), 50 μg/mL actinomycin D, and 500 μM each of ATP, CTP, GTP, and UTP (Roche Diagnostics, Basel, Switzerland) in buffer B (pH 7.7). Total RNA was purified by the acid guanidinium-phenol-chloroform method. In this assay, considering that the estimated SM content in human hepatocytes is 3–4 nmol/mg protein, as demonstrated by MS analysis (**Figure S10**), the amount of SM we added in the replicase assay was 0.3–1 μM. (i.e. 0.03–0.3 nmol/0.3 mL/0.1 mg protein/12 well; the reaction volume in the replicase assay was 0.3 mL/12 wells and each well of the 12 well cell culture plates contained approximately 0.1 mg protein.)

Statistical analysis

Statistical analysis was performed using the Student's *t*-test equipped with Excel 2008 (Microsoft, Redmond, WA, USA). To measure the strength of the association, Pearson correlation coefficient was calculated using Excel 2008. A p-value<0.05 was considered statistically significant.

Supporting Information

Figure S1 Impacts of HBV infection on expression of sphingomyelin (SM) biosynthesis genes. mRNA expression of *SGMS1* and *SGMS2* genes (encoding SM synthases 1 and 2, respectively) in uninfected (white) and infected (black) chimeric mice (n = 5 per group).
(JPG)

Figure S2 Effect of HCV infection in cultured cells. Comparison of the relative amounts of SM, as measured by MS analysis, in mock-infected (HuH-7 K4 cells) (white) and HCV (JFH-1)-infected cells (JFH/K4 cells) (black) (n = 1 per group).
(JPG)

Figure S3 The expression of HCV core protein in HCV-infected chimeric mice. Histological analysis using immunohistochemical labeling of HCV core protein.
(JPG)

Figure S4 Effects of NA808 on HCV-infected chimeric mice. (**A**) Average body weight of mice during treatment. (**B**) Average human albumin concentrations in the sera of mice during

treatment. (**C**) Histological analysis using H&E staining and immunofluorescent labeling of human albumin (red). In all cases, error bars indicate SDs.
(JPG)

Figure S5 Concentrations of NA808 in chimeric mice receiving NA808 treatment. Concentration of NA808 in the liver (gray) and serum (black) of chimeric mice treated with 5 mg/kg or 10 mg/kg NA808. Stars indicate that NA808 level was not detected.
(JPG)

Figure S6 Sphingomyelin (SM) levels in the serum of chimeric mice receiving NA808 treatment. SM levels in the serum of chimeric mice (n = 3 per group) that were uninfected (HCV−), or infected (HCV+) but untreated or treated with 5 or 10 mg/kg NA808. Error bars indicate SDs.
(JPG)

Figure S7 Effects of NA808 on associations between the HCV nonstructural 5B polymerase (RdRp) and sphingomyelin (SM). (**A**) Comparison of SDS-PAGE and TLC results for replicon cells receiving no treatment (Control) or NA808 treatment (NA808). NA808 dosage was 2.5 nM (for TLC) or 25 nM (for SDS-PAGE). (**B**) Relative band intensities of RdRp and NS3 in detergent-resistant membrane (DRM) fractions from cells receiving no treatment (Control) or 25 nM NA808 treatment (NA808). (**C**) Relative band intensities of SM in DRM fractions from cells receiving no treatment (Control) or 2.5 nM NA808 treatment (NA808).
(JPG)

Figure S8 Composition ratio of SM molecular species in whole cells and DRM fraction of uninfected cells.
(JPG)

Figure S9 Effect of NS3 protease inhibitor on SM molecular species in the DRM fractions of subgenomic replicon cells. (A) Effect of NS3 protease inhibitor (VX950) on HCV replication (dark grey bars) and cell viability (light grey bars) in FLR3-1 replicon-containing cells. Error bars indicate SD. (B) Effect of NS3 protease inhibitor (VX950; 3 μM) on SM molecular species of DRM fractions of FLR 3-1 replicon-containing cells. Error bars indicate SDs.
(JPG)

Figure S10 The estimated SM content in human hepatocytes. Left bar (white) indicates the intensity of SM internal standard (SM d18:0-12:0; 1 nmol) by mass spectrometer. Right bar indicates the intensity of 1 mg protein of human hepatocyte (HuH-7 K4).
(JPG)

Table S1 Distribution of radioactivity in tissues after a single intravenous administration of [^{14}C] NA808 at 2 mg/kg to non-fasting male rats.
(PDF)

Table S2 Treatment administration for HCV-infected chimeric mice. Administration of reagents was started at day 0. The amount of NA808 was adjusted according to the body weight of the mice. Dose began at 5 mg/kg or 10 mg/kg and was reduced by half at each 10% reduction in body weight (half circle). At 20% reduction, administration was discontinued. Open circle indicates each manipulation was performed as required.
(PDF)

Text S1 Materials and methods for supporting information. Methods for "Infection of chimeric mice with hepatitis B virus", "Quantification of human albumin", "Histological staining and indirect immunofluorescence analysis", and "Quantification of sphingomyelin (SM) in serum" are described.
(DOCX)

Acknowledgments

We are very grateful to Dr. Makoto Hijikata of the Department of Viral Oncology, Institute for Virus Research, Kyoto University for his technical support. We thank Isao Maruyama and Hiroshi Yokomichi of PhoenixBio Co., Ltd. for maintenance of and technical assistance with the chimeric mice.

Author Contributions

Conceived and designed the experiments: M. Kohara. Wrote the paper: Y. Hirata. Y. Hirata performed the experiment of chimeric mice and HCV-infected cells. K. Ikeda, M. Ohta, T. Soga, and R. Taguchi performed lipid analysis by MS spectrometry. M. Sudoh, A. Katsume, and Y. Aoki evaluated the antiviral effects of NA808, K. Okano and K. Ozeki examined the tissue distribution of NA808. K. Kawasaki and T. Tsukuda synthesized derivatives from natural compounds. Y. Tokunaga, Y. Tobita, T. Umehara, and S. Sekiguchi performed some experiments on the chimeric mice. L. Weng and T. Toyoda conducted the experiments on the interaction between RdRp and SM. M. Kohara and Y. Hirata performed data analysis on the chimeric mice and cells. K. Ikeda, M. Ohta, T. Soga, and R. Taguchi performed data analysis on the result of MS spectrometry. A. Suzuki, K. Shimotohno, and M. Nishijima provided tools and expert information.

References

1. Wenk MR (2006) Lipidomics of host-pathogen interactions. FEBS Lett 580: 5541–5551.
2. Brown DA, Rose JK (1992) Sorting of GPI-anchored proteins to glycolipid-enriched membrane subdomains during transport to the apical cell surface. Cell 68: 533–544.
3. Simons K, Toomre D (2000) Lipid rafts and signal transduction. Nat Rev Mol Cell Biol 1: 31–39.
4. van der Meer-Janssen YP, van Galen J, Batenburg JJ, Helms JB (2010) Lipids in host-pathogen interactions: pathogens exploit the complexity of the host cell lipidome. Prog Lipid Res 49: 1–26.
5. Aizaki H, Lee KJ, Sung VM, Ishiko H, Lai MM (2004) Characterization of the hepatitis C virus RNA replication complex associated with lipid rafts. Virology 324: 450–461.
6. Shi ST, Lee KJ, Aizaki H, Hwang SB, Lai MM (2003) Hepatitis C virus RNA replication occurs on a detergent-resistant membrane that cofractionates with caveolin-2. J Virol 77: 4160–4168.
7. Sakamoto H, Okamoto K, Aoki M, Kato H, Katsume A, et al. (2005) Host sphingolipid biosynthesis as a target for hepatitis C virus therapy. Nat Chem Biol 1: 333–337.
8. Weng L, Hirata Y, Arai M, Kohara M, Wakita T, et al. (2010) Sphingomyelin activates hepatitis C virus RNA polymerase in a genotype-specific manner. J Virol 84: 11761–11770.
9. Umehara T, Sudoh M, Yasui F, Matsuda C, Hayashi Y, et al. (2006) Serine palmitoyltransferase inhibitor suppresses HCV replication in a mouse model. Biochem Biophys Res Commun 346: 67–73.
10. Kapadia SB, Chisari FV (2005) Hepatitis C virus RNA replication is regulated by host geranylgeranylation and fatty acids. Proc Natl Acad Sci U S A 102: 2561–2566.
11. Su AI, Pezacki JP, Wodicka L, Brideau AD, Supekova L, et al. (2002) Genomic analysis of the host response to hepatitis C virus infection. Proc Natl Acad Sci U S A 99: 15669–15674.
12. Takano T, Tsukiyama-Kohara K, Hayashi M, Hirata Y, Satoh M, et al. (2011) Augmentation of DHCR24 expression by hepatitis C virus infection facilitates viral replication in hepatocytes. J Hepatol 55: 512–521.
13. Tateno C, Yoshizane Y, Saito N, Kataoka M, Utoh R, et al. (2004) Near completely humanized liver in mice shows human-type metabolic responses to drugs. Am J Pathol 165: 901–912.
14. Mercer DF, Schiller DE, Elliott JF, Douglas DN, Hao C, et al. (2001) Hepatitis C virus replication in mice with chimeric human livers. Nat Med 7: 927–933.

15. Valsecchi M, Mauri L, Casellato R, Prioni S, Loberto N, et al. (2007) Ceramide and sphingomyelin species of fibroblasts and neurons in culture. J Lipid Res 48: 417–424.
16. Watanabe T, Sudoh M, Miyagishi M, Akashi H, Arai M, et al. (2006) Intracellular-diced dsRNA has enhanced efficacy for silencing HCV RNA and overcomes variation in the viral genotype. Gene Ther 13: 883–892.
17. Fujita T, Inoue K, Yamamoto S, Ikumoto T, Sasaki S, et al. (1994) Fungal metabolites. Part 11. A potent immunosuppressive activity found in Isaria sinclairii metabolite. J Antibiot (Tokyo) 47: 208–215.
18. Miyake Y, Kozutsumi Y, Nakamura S, Fujita T, Kawasaki T (1995) Serine palmitoyltransferase is the primary target of a sphingosine-like immunosuppressant, ISP-1/myriocin. Biochem Biophys Res Commun 211: 396–403.
19. Park TS, Panek RL, Mueller SB, Hanselman JC, Rosebury WS, et al. (2004) Inhibition of sphingomyelin synthesis reduces atherogenesis in apolipoprotein E-knockout mice. Circulation 110: 3465–3471.
20. Miyanari Y, Hijikata M, Yamaji M, Hosaka M, Takahashi H, et al. (2003) Hepatitis C virus non-structural proteins in the probable membranous compartment function in viral genome replication. J Biol Chem 278: 50301–50308.
21. Diamond DL, Jacobs JM, Paeper B, Proll SC, Gritsenko MA, et al. (2007) Proteomic profiling of human liver biopsies: hepatitis C virus-induced fibrosis and mitochondrial dysfunction. Hepatology 46: 649–657.
22. Tardif KD, Mori K, Siddiqui A (2002) Hepatitis C virus subgenomic replicons induce endoplasmic reticulum stress activating an intracellular signaling pathway. J Virol 76: 7453–7459.
23. Pettus BJ, Chalfant CE, Hannun YA (2002) Ceramide in apoptosis: an overview and current perspectives. Biochim Biophys Acta 1585: 114–125.
24. Tepper AD, Ruurs P, Wiedmer T, Sims PJ, Borst J, et al. (2000) Sphingomyelin hydrolysis to ceramide during the execution phase of apoptosis results from phospholipid scrambling and alters cell-surface morphology. J Cell Biol 150: 155–164.
25. Liu YY, Han TY, Giuliano AE, Hansen N, Cabot MC (2000) Uncoupling ceramide glycosylation by transfection of glucosylceramide synthase antisense reverses adriamycin resistance. J Biol Chem 275: 7138–7143.
26. Taguchi Y, Kondo T, Watanabe M, Miyaji M, Umehara H, et al. (2004) Interleukin-2-induced survival of natural killer (NK) cells involving phosphatidylinositol-3 kinase-dependent reduction of ceramide through acid sphingomyelinase, sphingomyelin synthase, and glucosylceramide synthase. Blood 104: 3285–3293.
27. Diamond DL, Syder AJ, Jacobs JM, Sorensen CM, Walters KA, et al. (2010) Temporal proteome and lipidome profiles reveal hepatitis C virus-associated reprogramming of hepatocellular metabolism and bioenergetics. PLoS Pathog 6: e1000719.
28. Huitema K, van den Dikkenberg J, Brouwers JF, Holthuis JC (2004) Identification of a family of animal sphingomyelin synthases. EMBO J 23: 33–44.
29. Merrill AH, Jr., Schmelz EM, Dillehay DL, Spiegel S, Shayman JA, et al. (1997) Sphingolipids–the enigmatic lipid class: biochemistry, physiology, and pathophysiology. Toxicol Appl Pharmacol 142: 208–225.
30. Huwiler A, Kolter T, Pfeilschifter J, Sandhoff K (2000) Physiology and pathophysiology of sphingolipid metabolism and signaling. Biochim Biophys Acta 1485: 63–99.
31. Hannun YA, Luberto C, Argraves KM (2001) Enzymes of sphingolipid metabolism: from modular to integrative signaling. Biochemistry 40: 4893–4903.
32. van Genderen IL, Brandimarti R, Torrisi MR, Campadelli G, van Meer G (1994) The phospholipid composition of extracellular herpes simplex virions differs from that of host cell nuclei. Virology 200: 831–836.
33. Brugger B, Glass B, Haberkant P, Leibrecht I, Wieland FT, et al. (2006) The HIV lipidome: a raft with an unusual composition. Proc Natl Acad Sci U S A 103: 2641–2646.
34. Aizaki H, Morikawa K, Fukasawa M, Hara H, Inoue Y, et al. (2008) Critical role of virion-associated cholesterol and sphingolipid in hepatitis C virus infection. J Virol 82: 5715–5724.
35. Syed GH, Amako Y, Siddiqui A (2010) Hepatitis C virus hijacks host lipid metabolism. Trends Endocrinol Metab 21: 33–40.
36. Berger KL, Cooper JD, Heaton NS, Yoon R, Oakland TE, et al. (2009) Roles for endocytic trafficking and phosphatidylinositol 4-kinase III alpha in hepatitis C virus replication. Proc Natl Acad Sci U S A 106: 7577–7582.
37. Borawski J, Troke P, Puyang X, Gibaja V, Zhao S, et al. (2009) Class III phosphatidylinositol 4-kinase alpha and beta are novel host factor regulators of hepatitis C virus replication. J Virol 83: 10058–10074.
38. Tai AW, Benita Y, Peng LF, Kim SS, Sakamoto N, et al. (2009) A functional genomic screen identifies cellular cofactors of hepatitis C virus replication. Cell Host Microbe 5: 298–307.
39. Vaillancourt FH, Pilote L, Cartier M, Lippens J, Liuzzi M, et al. (2009) Identification of a lipid kinase as a host factor involved in hepatitis C virus RNA replication. Virology 387: 5–10.
40. Amemiya F, Maekawa S, Itakura Y, Kanayama A, Matsui A, et al. (2008) Targeting lipid metabolism in the treatment of hepatitis C virus infection. J Infect Dis 197: 361–370.
41. Ishitsuka R, Sato SB, Kobayashi T (2005) Imaging lipid rafts. J Biochem 137: 249–254.
42. Ramstedt B, Slotte JP (2002) Membrane properties of sphingomyelins. FEBS Lett 531: 33–37.
43. He Q, Suzuki H, Sharma N, Sharma RP (2006) Ceramide synthase inhibition by fumonisin B1 treatment activates sphingolipid-metabolizing systems in mouse liver. Toxicol Sci 94: 388–397.
44. Bligh EG, Dyer WJ (1959) A rapid method of total lipid extraction and purification. Can J Biochem Physiol 37: 911–917.
45. Inoue K, Umehara T, Ruegg UT, Yasui F, Watanabe T, et al. (2007) Evaluation of a cyclophilin inhibitor in hepatitis C virus-infected chimeric mice in vivo. Hepatology 45: 921–928.
46. Kashiwakuma T, Hasegawa A, Kajita T, Takata A, Mori H, et al. (1996) Detection of hepatitis C virus specific core protein in serum of patients by a sensitive fluorescence enzyme immunoassay (FEIA). J Immunol Methods 190: 79–89.
47. Ikeda K, Shimizu T, Taguchi R (2008) Targeted analysis of ganglioside and sulfatide molecular species by LC/ESI-MS/MS with theoretically expanded multiple reaction monitoring. J Lipid Res 49: 2678–2689.
48. Taguchi R, Nishijima M, Shimizu T (2007) Basic analytical systems for lipidomics by mass spectrometry in Japan. Methods Enzymol 432: 185–211.
49. Ikeda K, Oike Y, Shimizu T, Taguchi R (2009) Global analysis of triacylglycerols including oxidized molecular species by reverse-phase high resolution LC/ESI-QTOF MS/MS. J Chromatogr B Analyt Technol Biomed Life Sci 877: 2639–2647.
50. Ikeda K, Mutoh M, Teraoka N, Nakanishi H, Wakabayashi K, et al. (2011) Increase of oxidant-related triglycerides and phosphatidylcholines in serum and small intestinal mucosa during development of intestinal polyp formation in Min mice. Cancer Sci 102: 79–87.

J Gastroenterol
DOI 10.1007/s00535-012-0676-y

ORIGINAL ARTICLE—LIVER, PANCREAS, AND BILIARY TRACT

Kinetics of peripheral hepatitis B virus-specific CD8$^+$ T cells in patients with onset of viral reactivation

Jun Aoki · Yuka Kowazaki · Takahiro Ohtsuki · Rumiko Okamoto · Kazuteru Ohashi · Seishu Hayashi · Hisashi Sakamaki · Michinori Kohara · Kiminori Kimura

Received: 16 May 2012 / Accepted: 21 August 2012

Abstract
Background Patients with resolved hepatitis B virus (HBV) infection undergoing chemotherapy or immunosuppressive therapy are potentially at risk of HBV reactivation. However, it remains unclear how liver disease develops after HBV reactivation. To compare the host immune response against HBV, we performed immunological analyses of six HBV reactivation patients.
Methods The numbers of peripheral HBV-specific CD8$^+$ T cells were investigated longitudinally in six HLA-A2- and/or A24-positive patients with HBV reactivation. In addition, 34 patients with resolved HBV, 17 patients with inactive chronic hepatitis B (ICHB), 17 patients with chronic hepatitis B (CHB) and 12 healthy controls were analyzed. The number and function of HBV-specific CD8$^+$ T cells were assessed by flow cytometry using tetramer staining and intracellular IFN-γ production. Furthermore, the numbers of CD4$^+$CD25$^+$ or CD4$^+$Foxp3$^+$ T cells and serum inflammatory cytokine levels were analyzed.
Results The frequency of HBV-specific CD8$^+$ T cells was significantly increased in HBV reactivation patients compared with ICHB and CHB patients. In addition, the number of HBV-specific CD8$^+$ T cells was increased in resolved HBV patients compared with ICHB patients. PD-1 expression was decreased in HBV reactivation patients compared with ICHB and CHB patients. The numbers of HBV-specific CD8$^+$ T cells and CD4$^+$CD25$^+$ or CD4$^+$Foxp3$^+$ T cells were negatively correlated following onset of HBV reactivation.
Conclusions During HBV reactivation, the frequency of HBV-specific CD8$^+$ T cells increased even though the administration of immunosuppressive drugs and interactions with CD4$^+$ regulatory T cells may be important for the onset of liver disease.

Keywords Hepatitis B virus reactivation · Cytotoxic T lymphocyte · Regulatory T cell · PD-1

Abbreviations

HBV	Hepatitis B virus
CTL	Cytotoxic T lymphocyte
sALT	Serum alanine aminotransferase
TNF	Tumor necrosis factor
IFN	Interferon
MIP	Macrophage inflammatory protein
MCP	Monocyte chemotactic protein

Electronic supplementary material The online version of this article (doi:10.1007/s00535-012-0676-y) contains supplementary material, which is available to authorized users.

J. Aoki · K. Ohashi · H. Sakamaki
Division of Hematology, Tokyo Metropolitan Cancer and Infectious Diseases Center, Komagome Hospital, 18-22-3 Honkomagome, Bunkyo-ku, Tokyo 113-8677, Japan

Y. Kowazaki · S. Hayashi · K. Kimura (✉)
Division of Hepatology, Tokyo Metropolitan Cancer and Infectious Diseases Center, Komagome Hospital, 18-22-3 Honkomagome, Bunkyo-ku, Tokyo 113-8677, Japan
e-mail: kkimura@cick.jp

T. Ohtsuki · M. Kohara · K. Kimura
Department of Microbiology and Cell Biology, Tokyo Metropolitan Institute of Medical Science, 2-1-6 Kamikitazawa, Setagaya-ku, Tokyo 156-8506, Japan

R. Okamoto
Division of Chemotherapy, Tokyo Metropolitan Cancer and Infectious Diseases Center, Komagome Hospital, 18-22-3 Honkomagome, Bunkyo-ku, Tokyo 113-8677, Japan

Published online: 26 September 2012

Introduction

More than 300 million people worldwide suffer from persistent hepatitis B virus (HBV) infection, making the virus a common cause of morbidity and mortality [1, 2]. Each year, an estimated one million people die of complications associated with chronic HBV infection, including cirrhosis, end-stage liver disease and hepatocellular carcinoma [3, 4]. Viral reactivation in hepatitis B surface antigen (HBsAg) carriers undergoing immunosuppressive therapy is well documented, as some immunosuppressive therapies can enhance HBV replication in hepatocytes at the same time as they curb host immune responses, resulting in detectable viremia followed by clinical hepatitis [1]. In general, although the development of surface and core antibodies and loss of surface antigen following HBV infection are thought to represent clearance of the virus, evidence exists to support the possibility that the virus may remain latent within the liver [5, 6]. The course and outcome of HBV infection are modulated by the host immune response [7, 8], and the loss of immune surveillance can cause reactivation of viral replication and exacerbation of disease activity. HBV reactivation is a well-characterized syndrome marked by the abrupt reappearance or elevation of HBV DNA in the serum of a patient with previously inactive or resolved HBV infection [1, 9]. Although the mechanisms of reactivation and associated liver damage remain unclear, they may include a rebound increase in the lymphocyte number following cessation of immunosuppressive and myelosuppressive chemotherapy, leading to a rapid destruction of infected hepatocytes with subsequent severe hepatitis. As one of the viral factors, it has been reported that the fulminant outcome of HBV reactivation can be associated with genotype Bj, which exhibits high replication owing to the A1896 mutation [10]. Therefore, although there are increasing reports regarding viral factors for the mechanism of HBV reactivation, it is still premature to conclude how the host immune response affects the liver injury and viral load.

It has been demonstrated that chronic persistent HBV infection is manifested by cytotoxic T lymphocytes (CTLs) that are functionally impaired or exhausted [7]. Recent reports have indicated that PD-1 is markedly upregulated on the surface of exhausted virus-specific $CD8^+$ T cells in mice with lymphocytic choriomeningitis virus infection [11] and humans with human immunodeficiency virus (HIV) infection [12, 13] or hepatitis C virus (HCV) infection [14]. Based on these observations, we evaluated the hypothesis that HBV-specific $CD8^+$ T cells can restore their function during HBV reactivation, by analyzing PD-1 expression on HBV-specific $CD8^+$ T cells. In a previous report, we demonstrated that fulminant hepatitis in HBV patients was responsible for high amounts of interferon (IFN)-γ production by $CD8^+$ T cells from peripheral blood mononuclear cells (PBMCs) [15]. Thus, HBV-specific $CD8^+$ T cells may be responsible for the liver disease at the onset of HBV reactivation, although a causal relationship among these events has not been defined.

In this study, we found that the frequency of HBV-specific $CD8^+$ T cells was increased and the interactions between these $CD8^+$ T cells and $CD4^+$ regulatory T cells (Tregs) showed a negative correlation at the onset of HBV reactivation.

Patients and methods

Patients

Six patients with HBV reactivation from resolved HBV infection before chemotherapy or immunosuppressive therapy, 34 patients with resolved HBV, 17 patients with inactive chronic hepatitis B (ICHB), 17 patients with chronic hepatitis B (CHB) and 12 healthy controls gave informed consent to participate in the study. The study was performed at Tokyo Metropolitan Komagome Hospital after receiving institutional review board approval (approved ID number: 714). We defined resolved HBV infection as serum HBsAg (−), anti-HBcAb (+) and/or anti-HBsAb (+), ICHB as serum HBsAg (+), HBV DNA (+) and normal serum alanine aminotransferase (sALT; 5–40 IU/mL), and CHB as serum HBsAg (+), HBV DNA (+) and continuous serum ALT elevation (>2 × normal level). The study protocol and procedures were conducted in accordance with the ethical guidelines of the Declaration of Helsinki. The patient characteristics are summarized in Table 1. The healthy controls comprised six males and six females, who ranged in age from 32 to 63 years. There were no significant differences in age between the HBV reactivation patients and the other groups. The patients were human leukocyte antigen (HLA)-A2- or A24-positive and negative for HCV and HIV-1/2.

Sample preparation

PBMCs were isolated from whole blood using Lymphoprep™ (Axis-Shield, Oslo, Norway). The isolated cells were washed twice in phosphate-buffered saline (Gibco, Auckland, NZ) and used immediately. The cells were cultured in RPMI 1640 medium supplemented with 10 % heat-inactivated fetal calf serum, 100 U/mL penicillin, 100 mg/mL streptomycin, 50 μg/mL gentamicin and 2 mM L-glutamine (all from Invitrogen, Carlsbad, CA) at 37 °C in a humidified 5 % CO_2 incubator, as previously described [15]. Plasma preparation tubes (BD Biosciences, San Jose, CA) were used to isolate plasma from whole

Table 1 Characteristics of the respective patient groups

	Number	Sex (M/F)	Age	ALT (U/L)	HBV DNA (log/mL)
Healthy volunteer	12	6/6	57 ± 11	25 ± 11	–
Resolved HBV	34	18/16	59 ± 15	33 ± 20	–
ICHB	17	8/9	55 ± 14	33 ± 14	3.9 ± 1.8
CHB	17	8/9	53 ± 11	75 ± 19	5.5 ± 1.9
Reactivation	6	3/3	66 ± 12	82 ± 66	5.8 ± 3.3

Results are shown as mean ± SD

ALT alanine transaminase, *ICHB* inactive chronic hepatitis B, *CHB* chronic hepatitis B, *HBV* hepatitis B virus, *M* male, *F* female

blood. The plasma samples were frozen and subsequently thawed for viral load and genotype testing.

Synthetic peptides

Three HBV peptides; HLA-A*0201 core 18–27 (FLPSDFFPSV), envelope 183–191 (FLLTRILTI), polymerase 575–583 (FLLSLGIHL), HLA-A*2402 core 117–125 (EYLVSFGVW), polymerase 756–764 (KYTSFPWLL) and were synthesized by Sigma Aldrich (Hokkaido, Japan).

Major histocompatibility complex (MHC) class I tetramer staining

Patients expressing HLA-A2 or A24 were assessed for antigen-specific responses to HBV by tetramer staining. For the staining, phycoerythrin (PE)-conjugated HLA-A*0201-restricted HBV core (FLPSDFFPSV) and HLA-A*2402 HBV core (EYLVSFGVW) HBV polymerase (KYTSFPWLL) were purchased from MBL (Nagoya, Japan).

FACS analysis

HLA typing was performed by staining PBMCs with fluorescein isothiocyanate (FITC)-conjugated anti-HLA-A2 and PE-conjugated anti-HLA-A24 antibodies (MBL) according to the manufacturer's instructions. PBMCs were surface-stained on ice for 20 min with the following monoclonal antibodies: FITC-conjugated anti-human CD62L, anti-PD-1 and anti-CD25 (BD Biosciences); PE-conjugated anti-human Foxp3 (eBioscience, San Diego, CA); and PE-Cy5-conjugated anti-human CD4 and anti-human CD8 (BD Biosciences). For intracellular staining, isolated PBMCs were incubated with peptides (10 μl/mL) in the presence of human recombinant IL-2 (50 U/mL) and 1 μl/mL of BD GolgiPlug protein transport inhibitor (BD Bioscience) for 4 h. After incubation (37 °C, 5 % CO_2), cells from each well were stained with PE-Cy5-conjugated anti-human CD8 (BD Biosciences). Prior to staining with intracellular antibodies against PE-conjugated anti-human IFN-γ, cells were fixed and permeabilized by adding Cytofix-Cytoperm (BD Pharmingen). Cells were acquired by FACS scan (BD Biosciences), and the data was analyzed using FlowJo software (Tree Star, Ashland, OR).

Cytokine and chemokine profiles

Bio-Plex Cytokine Assay Kits (Bio-Rad Laboratories, Hercules, CA) were used to measure the amounts of cytokines and chemokines in sera in accordance with the manufacturer's instructions. Specifically, we used the Bio-Plex Human Cytokine 17-Plex Panel. The resulting samples were analyzed in a 96-well plate reader using a Bio-Plex Suspension Array System and Bio-Plex Manager software (all from Bio-Rad Laboratories).

Serum HBV assay

The serum HBV DNA concentrations were quantified using the COBAS AmpliPrep/COBAS TaqMan HBV Test (Roche Diagnostics, Basel, Switzerland). The four major HBV genotypes (A–D) were determined by enzyme-linked immunosorbent assay with monoclonal antibodies directed against distinct epitopes on the preS2-region products using commercial kits (HBV GENOTYPE EIA; Institute of Immunology Co. Ltd., Tokyo, Japan). HBV DNA sequences bearing the core promoter and precore or core regions were amplified by PCR with hemi-nested primers. The PCR products were directly sequenced by the di-deoxy-chain termination method using a Big Dye Terminator Kit and an ABI PRISM 3100-Avant Analyzer (both from Applied Biosystems, Foster City, CA).

Statistical analysis

Data are shown as mean ± SD. The data were analyzed by the nonparametric Mann–Whitney or Kruskal–Wallis tests or ANOVA using Prism 5 for Macintosh software (GraphPad, San Diego, CA). Values of $P < 0.05$ were considered to indicate statistical significance.

Table 2 Characteristics of HBV reactivation patients

Patient	Sex	Disease	HBsAg	HBsAb	HBcAb	Chemotherpy/ Immunosuppressant	HBV genotype	HBVcore/precore mutation
#1	Female	ALL, BMT	−	+	+	PSL, FK	C	−
#2	Male	AML, BMT	−	+	+	PSL, CsA	C	−
#3	Male	Eso.ca	−	+	+	5FU + CDDP	C	−
#4	Male	B cell lymphoma	−	+	+	R-CHOP	B	−
#5	Male	B cell lymphoma	−	+	+	CHOP	B	−
#6	Female	T-LBL, BMT	−	+	+	Anthracycline + AraC	B	−

ALL acute lymphoblastic leukemia, *BMT* bone marrow transplantation, *PSL* prednisolone, *FK* tacrolimus, *CsA* ciclosporin A, *CDDP* cisplatin, *5FU* 5-fluorouracil, *R-CHOP* rituximab, cyclophosphamide, doxorubicin hydrochloride (hydroxydaunorubicin), vincristine (oncovin), and prednisone, *AraC* cytarabine

Results

HBV reactivation patient profiles

We identified six patients with HBV reactivation (Table 2). Patients with malignant lymphoma and bone marrow transplantation for leukemia were observed, and treatment with rituximab, which is a well-known inducer of HBV reactivation, was encountered in the case of one patient (patient #4). There was no sex difference regarding the incidence of HBV reactivation. All patients were negative for HBsAg and positive for anti-HBc and anti-HBs antibodies as HBV-related markers. In addition, three patients were HBV genotype C and one patient was genotype B. No core and precore promoter mutations were detected in the patients. All patients received entecavir (0.5 mg/day) when serum HBV DNA was initially detected or sALT elevation was observed.

Serum inflammatory cytokine and chemokine levels

To determine whether the serum cytokine and chemokine levels correlated with the development of HBV reactivation, we examined the concentrations of various cytokines and chemokines. We measured serum cytokine/chemokine levels at the time of diagnosis of HBV reactivation. In the groups, serum was isolated prior to chemotherapy or antiviral therapy.

The data for the serum cytokine and chemokine levels are shown in Fig. 1. Serum IL-1β was significantly higher in resolved HBV patients (median, 0.32 pg/mL; range 0.10–0.75 pg/mL) than in healthy controls (median, 0.17 pg/mL; range 0.04–0.43 pg/mL) or ICHB patients (median, 0.17 pg/mL; range 0.09–0.24 pg/mL). Serum IL-7 was elevated in resolved HBV patients (median, 6.4 pg/mL; range 0.54–28.12 pg/mL) compared with ICHB patients (median, 3.2 pg/mL; range 0.54–12.6 pg/mL) or CHB patients (median, 3.13 pg/mL; range 0.29–5.16 pg/mL). There were no significant differences in serum IL-6 among resolved HBV, ICHB, CHB and HBV reactivation patients. Serum IL-8 and MCP-1 were significantly increased in resolved HBV patients (IL-8: median, 12.5 pg/mL; range 5.15–34.2 pg/mL; MCP-1: median, 75.2 pg/mL; range 0.7–300.23 pg/mL) compared with healthy controls (IL-8: median, 5.24 pg/mL; range not detected–17.46 pg/mL; MCP-1: median, 23.3 pg/mL; range not detected–48.51 pg/mL) and CHB patients (IL-8: median, 7.25 pg/mL; range 1.13–23.84 pg/mL; MCP-1: median, 21.8 pg/mL; range 3.49–58.66 pg/mL). Although circulating IFN-γ was detected at very low levels in all samples, ICHB patients exhibited significant suppression of serum IFN-γ. Regarding HBV reactivation, serum G-CSF was slightly increased compared with healthy controls.

Comparison of HBV-specific $CD8^+$ T cell frequencies

The development of hepatitis with HBV infection is mediated by antigen-specific CTLs [7]. To compare the frequencies and phenotypes of HBV-specific $CD8^+$ T cells from PBMCs, 16 HLA-A2- and 19 HLA-A24-positive resolved HBV patients, 9 HLA-A2- and 11 HLA-A24-positive ICHB patients, 11 HLA-A2- and 13 HLA-A24-positive CHB patients, and four HLA-A2- and four HLA-A24-positive HBV reactivation patients were examined using a panel of three MHC class I tetramers containing frequently detected HBV epitopes (A2 core, amino acids 18–27; A24 core, amino acids 117–125; and A24 polymerase, amino acids 756–764) (Fig. 2a). The frequency of peripheral HLA-A2 core-specific $CD8^+$ T cells was significantly higher in HBV reactivation patients than in ICHB and CHB patients (Fig. 2b, upper panels). Interestingly, the frequencies of HLA-A2 core-specific $CD8^+$ cells were also significantly higher in resolved HBV patients than in ICHB patients, indicating that HBV-specific $CD8^+$ T cells are circulating even though serum HBV DNA was not detected. Consistent with these data,

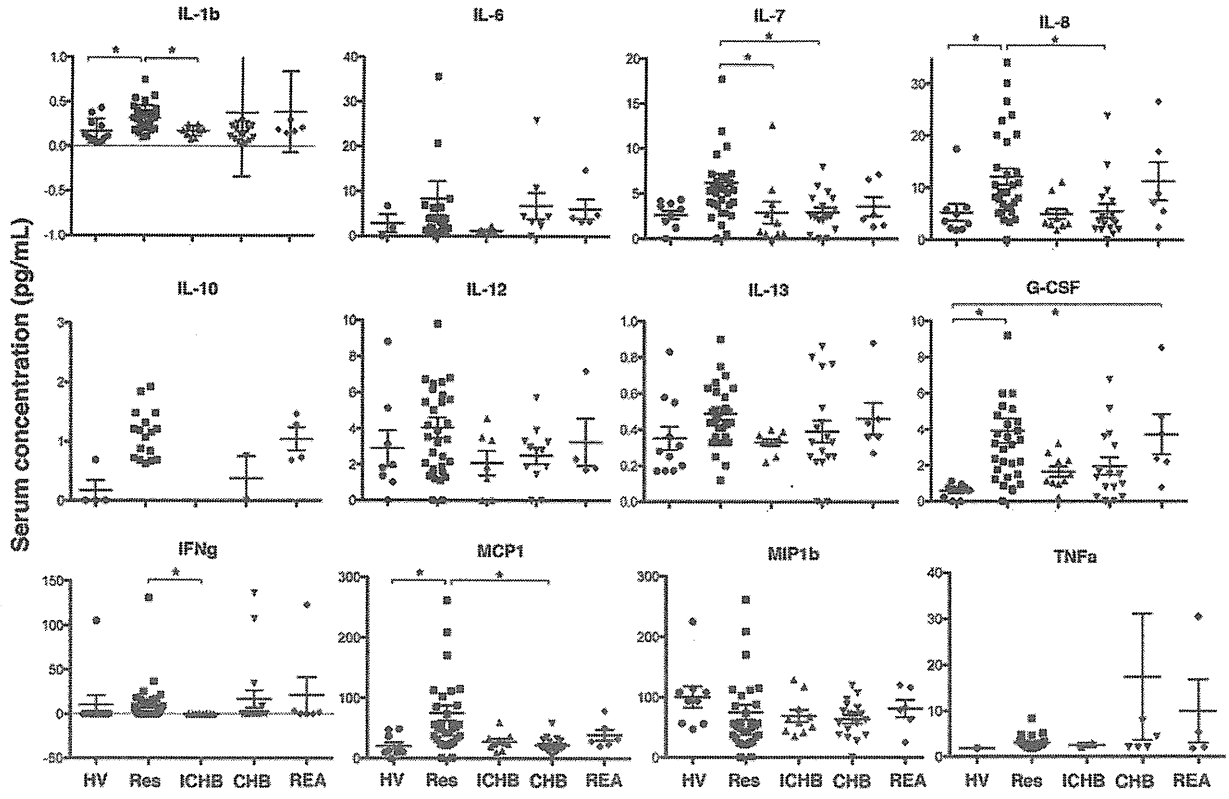

Fig. 1 Serum concentrations of cytokines and chemokines. Serum cytokines and chemokines were measured at the time of diagnosis in HBV reactivation patients and prior to chemotherapy or antiviral therapy in the other groups. The serum concentrations were compared among healthy controls, resolved HBV patients, ICHB patients, CHB patients and HBV reactivation patients. $^{*}P < 0.05$, significant difference between the linked items

the frequencies of HLA-A24 core- and polymerase-specific $CD8^+$ T cells were significantly higher in HBV reactivation patients than in ICHB and CHB patients.

In addition, to evaluate the functional profile of HBV-specific $CD8^+$ T cells we analyzed intracellular IFN-γ production following stimulation with five peptides. Although we did not observe a significant difference in the numbers of IFN-γ producing cells in HBV reactivation patients by HLA-A2 core peptide stimulation, similar results were obtained by tetramer staining following HLA-A24 core and polymerase stimulation (Fig. 2b). We also observed that the number of IFN-γ producing cells in HBV reactivation patients increased by HLA-A2 envelope peptide stimulation (supplementary Fig. 1). These results demonstrated that the frequency of functional HBV-specific $CD8^+$ T cells increased in HBV reactivation patients compared with ICHB and CHB patients.

It was demonstrated that the frequency of circulating $CD4^+CD25^+$ Tregs significantly correlated with the serum viral load in severe CHB patients [16]. To determine whether $CD4^+CD25^+$ and $CD4^+Foxp3^+$ Tregs contribute to liver injury during HBV reactivation, we monitored their numbers in PBMCs. The numbers of $CD4^+CD25^+$ and $CD4^+Foxp3^+$ Tregs had a tendency to be low in HBV reactivation patients compared with the other groups, although the differences were not significant (Fig. 2b, lower panels).

To confirm the inverse correlation between the percentages of HBV-specific $CD8^+$ T cells and the percentages of $CD4^+Foxp3^+$ T cells, we assessed these cells in all patients. As shown in Fig. 2c, a significant inverse correlation was not detected in all patients (white circles), whereas an inverse correlation was noted in HBV reactivation patients (black dots).

PD-1 and CD62L expression on HBV-specific and total $CD8^+$ T cells

The function of antigen-specific $CD8^+$ T cells is impaired, termed "exhaustion," during persistent chronic infection diseases like HBV [17], and exhausted antigen-specific $CD8^+$ T cells express high levels of PD-1 and low levels of CD62L [18]. Based on these findings, we evaluated the expression of PD-1 and CD62L on total $CD8^+$ T cells and

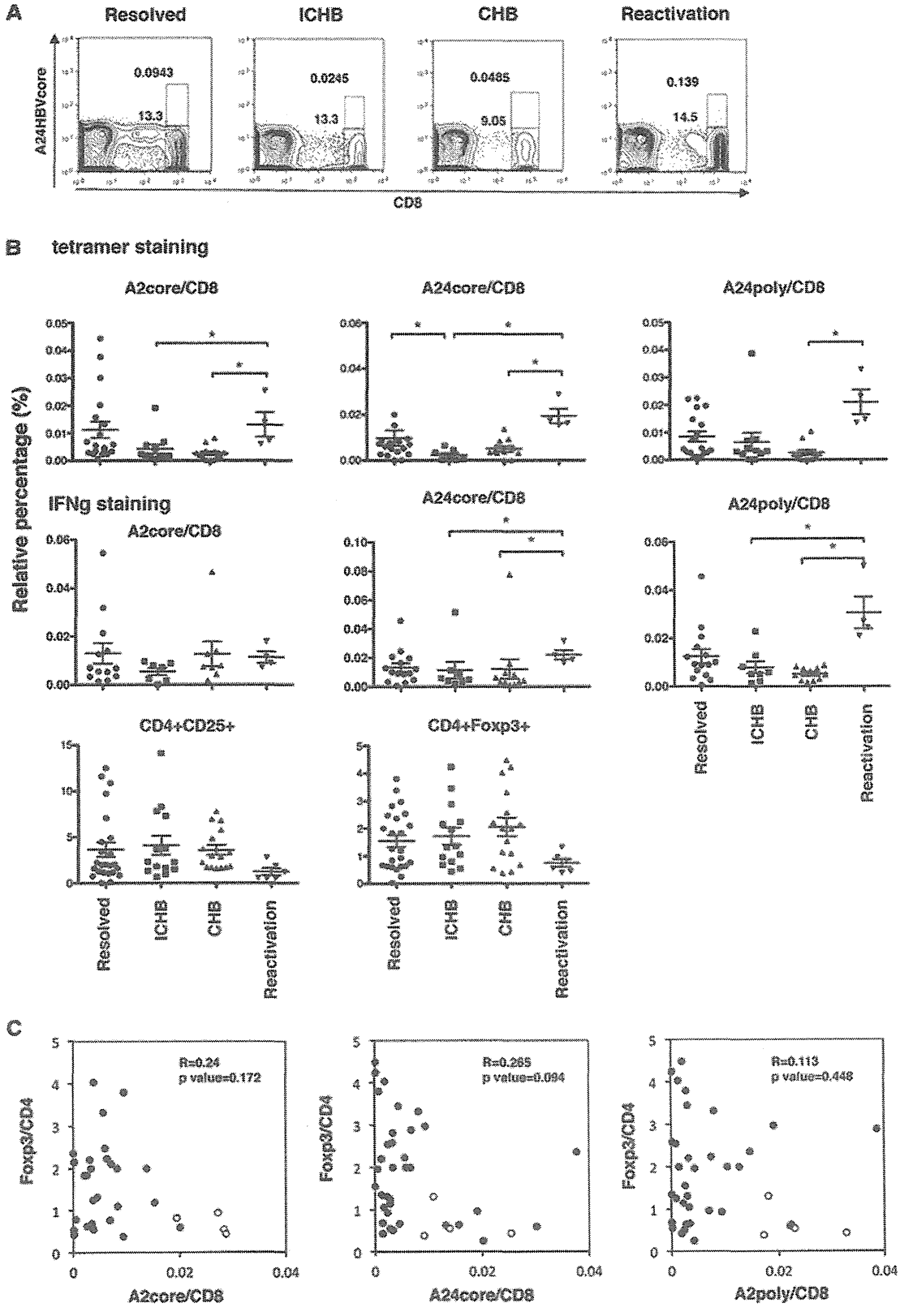
A
Resolved
ICHB
CHB
Reactivation
A24HBVcore
CD8
0.0943
13.3
0.0245
13.3
0.0485
9.05
0.139
14.5
B
tetramer staining
A2core/CD8
A24core/CD8
A24poly/CD8
Relative percentage (%)
IFNg staining
A2core/CD8
A24core/CD8
A24poly/CD8
CD4+CD25+
CD4+Foxp3+
Resolved
ICHB
CHB
Reactivation
C
Foxp3/CD4
R=0.24
p value=0.172
R=0.265
p value=0.094
R=0.113
p value=0.448
A2core/CD8
A24core/CD8
A2poly/CD8

◀ **Fig. 2** **a** FACS analysis using tetramer staining. To detect HBV specific CTLs in the PBMCs, we isolated PBMCs from 4 groups. The samples were stained with PE-conjugated anti-human HLA-A24 HBV core antibody and a PE-Cy5-conjugated anti-human CD8 antibody. **b** Frequencies of HBV-specific $CD8^+$ T cells and $CD4^+$ Tregs. The numbers of HBV-specific $CD8^+$ T cells and Tregs were analyzed by FACS at the time of diagnosis in HBV reactivation patients and prior to chemotherapy or antiviral therapy in the other groups. The *upper panels* show the percentages of HBV-specific $CD8^+$ T cells, among which the *left panel* shows the A2 core, the *center panel* shows the A24 core and the *right panel* shows A24 poly-specific $CD8^+$ T cells. The *middle panels* shows the percentage of IFN-γ producing $CD8^+$ T cells stimulated by peptides for A2 core, A24 core, and A24 poly, respectively. The *lower panels* show the percentages of Tregs, of which the *left panel* shows $CD4^+CD25^+$ Tregs and the *right panel* shows $CD4^+Foxp3^+$ Tregs. $*P < 0.05$, significant difference between the linked items. **c** Relationships between the frequencies of HBV-specific $CD8^+$ T cells and Tregs. The *scatter diagrams* show HBV reactivation patients (*white circle*) and other patients (*black dot*), respectively. The *left panel* shows the negative correlation between $CD4^+Foxp3^+$ Tregs and A2 core-specific $CD8^+$ T cells. The *center panel* shows the negative correlation between $CD4^+Foxp3^+$ Tregs and A24 core-specific $CD8^+$ T cells. The *right panel* shows the negative relationship between $CD4^+Foxp3^+$ Tregs and A24 poly-specific $CD8^+$ T cells

HBV-specific $CD8^+$ T cells to determine whether the $CD8^+$ T cell function in HBV reactivation patients was different from that in the other groups. Although PD-1 expression was higher on circulating HBV-specific $CD8^+$ T cells in ICHB and CHB patients, it was significantly lower on HBV-specific $CD8^+$ cells in HBV reactivation patients (Fig. 3). Curiously, PD-1 expression on HBV-specific $CD8^+$ T cells was low in resolved HBV patients compared with ICHB and CHB patients, indicating that HBV-specific $CD8^+$ T cells in resolved HBV patients may function in a similar manner to those in HBV reactivation patients.

It was also demonstrated that primary CD62L high expressing $CD8^+$ T cells were better at clearing LCMV infection compared with primary CD62L low expressing cells. In addition, CD62L high memory cells underwent robust expansion, and were efficient in preventing chronic LCMV infection [18]. Thus, to address the memory phenotype of cells we examined the expression of CD62L on HBV-specific $CD8^+$ T cells. However, we did not detect any significant differences in the expression of CD62L on $CD8^+$ T cells among the groups although CD62 expression in HBV reactivation patients had a tendency to be lower.

Longitudinal analysis of the frequencies of HBV-specific $CD8^+$ T cells and $CD4^+$ Tregs

To evaluate changes in the frequency of HBV-specific $CD8^+$ T cells during HBV reactivation, we monitored sALT levels, serum HBV DNA levels, percentages of HBV-specific $CD8^+$ T cells and numbers of $CD4^+CD25^+$ and $CD4^+Foxp3^+$ cells in the six HBV reactivation patients. As shown in Fig. 4, when serum HBV DNA was

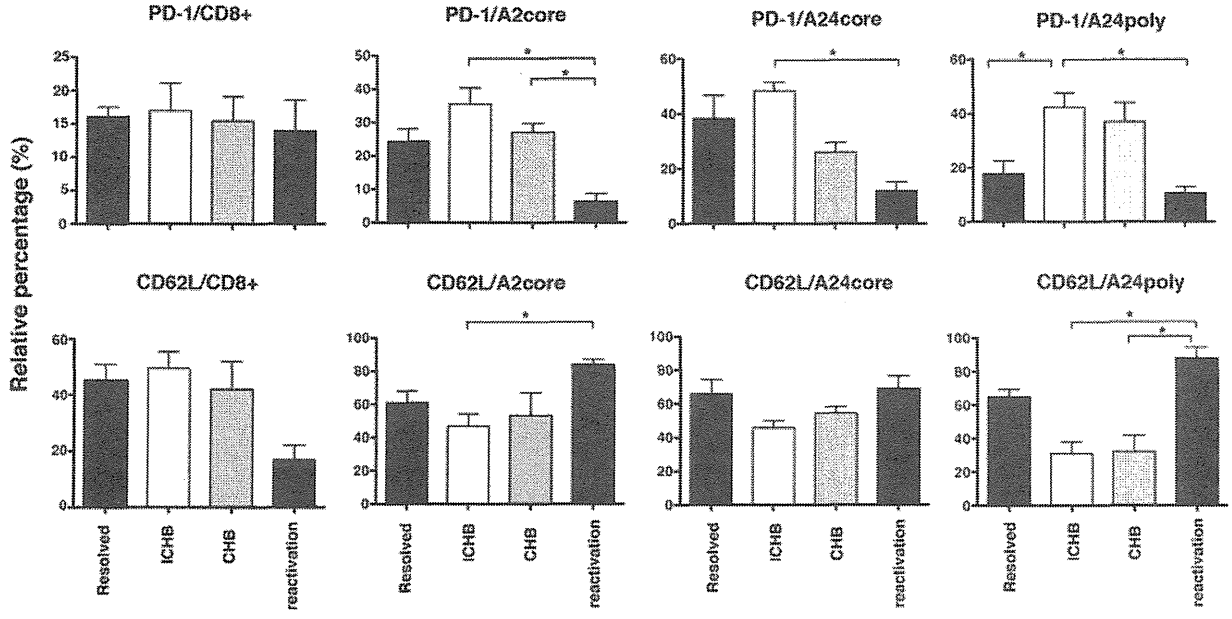

Fig. 3 PD-1 and CD62L expression in HBV-specific and total $CD8^+$ T cells. The PD-1 and CD62L expression levels in HBV-specific and total $CD8^+$ T cells were analyzed by FACS at the time of diagnosis in HBV reactivation patients and prior to chemotherapy or antiviral therapy in the other groups. The *left panel* shows the percentages of PD-1 or CD62L-positive cells in CD8 T^+ cells. The *three right panels* show PD-1 or CD62L-positive cells in HBV-specific $CD8^+$ T cells, respectively. $*P < 0.05$, significant difference between the linked items

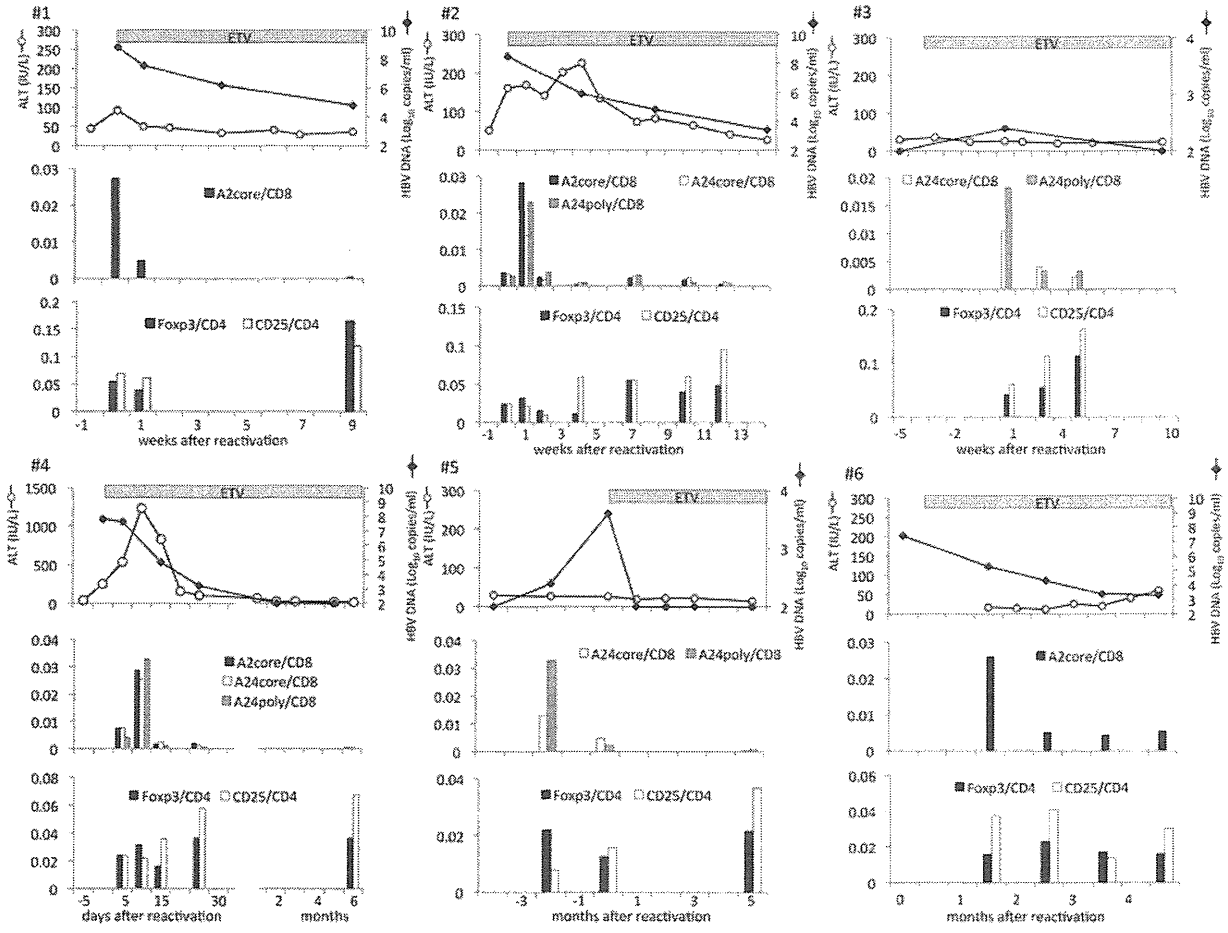

Fig. 4 Longitudinal analysis of the frequencies of HBV-specific $CD8^+$ T cells and Tregs. The *upper panels* show the kinetics of ALT (IU/L) (*white circle*) and HBV DNA (log_{10} copies/ml) (*black diamond*), the *middle panels* show the frequencies of HBV-specific $CD8^+$ T cells and the *lower panels* show the frequencies of Tregs, respectively. All patients were administered entecavir immediately following diagnosis

detected in resolved HBV patients, administration of entecavir was quickly started for all patients to prevent severe hepatitis. HBV-specific $CD8^+$ T cells were detected and reached their peak frequency levels at the onset of HBV reactivation in patients #1 to #6. Interestingly, a high percentage of HBV-specific $CD8^+$ T cells was observed in patient #4 compared with other patients and, consistent with this finding, the sALT level was markedly elevated to about 1200 IU/l, indicating that the number of HBV-specific $CD8^+$ T cells reflected the grade of liver damage, as previously reported [19]. Furthermore, when the numbers of HBV-specific $CD8^+$ T cells were maximal, the numbers of $CD4^+CD25^+$ and $CD4^+Foxp3^+$ T cells were minimal, indicating a negative correlation. Moreover, HBV-specific $CD8^+$ T cells decreased as the sALT level decreased, whereas $CD4^+CD25^+$ and $CD4^+Foxp3^+$ T cells showed tendencies to increase. However, the number of HBV-specific $CD8^+$ T cells in patient #6 did not decrease throughout the time course, although this patient showed tendencies for higher numbers of $CD4^+CD25^+$ and $CD4^+Foxp3^+$ T cells at the time of HBV reactivation. In this patient, the reduction in serum HBV DNA was slow and the sALT levels continued to be elevated. These findings suggest that $CD4^+$ Tregs may suppress an effective immune response against HBV.

Discussion

HBV reactivation is an almost universal event among patients with HBsAg undergoing bone marrow transplantation [20–22]. In retrospective analyses using sensitive serological and virological markers, a high proportion of people with anti-HBc antibodies without HBsAg in their serum also redevelop HBV DNA and HBsAg after bone marrow transplantation [23, 24]. In addition, the prolonged

impairment of immune-mediated control of intrahepatic HBV after extensive immunosuppression leads to reactivation of potential occult infection with HBsAg seroreversion [2]. Thus, although the risk of HBV reactivation during immunosuppression is well known, the mechanism for the induction of HBV reactivation is unclear.

In this study, we demonstrated that six patients with HBV reactivation showed increased numbers of HBV-specific $CD8^+$ T cells, similar to the case for self-limited acute hepatitis B, and that these T cells induced liver damage despite immunosuppression following treatment with an immunosuppressant and anti-cancer drug.

These findings are consistent with a previous report of a strong multifaceted CTL response in patients with acute hepatitis [7]. It is interesting to evaluate the function of antigen-specific $CD8^+$ T cells, including their proliferation and cytokine production, during immunosuppressive drug treatment, because a previous study showed that FK506 did not prevent the generation and proliferation of LCMV-specific T cells, but instead altered their differentiation so that these effector T cells lost their ability to control the virus [25]. Although we analyzed the role of $CD8^+$ T cells under the immunosuppressive status, it seems to be important to analyze macrophages, which produce TNF-α and IL-6 [25].

We found that the ratio of HBV-specific $CD8^+$ T cells was higher in resolved HBV patients than in ICHB and CHB patients, indicating that high viral loads suppress the frequency of these cells [26]. Furthermore, we showed that PD-1 expression on HBV-specific $CD8^+$ T cells was low in resolved HBV patients compared with ICHB and CHB patients, demonstrating that these cells can restore their function. These findings suggested that resolved HBV patients have numerous and functionally recovered HBV-specific $CD8^+$ T cells, and therefore, they may easily develop severe hepatitis once HBV reactivation is induced. This hypothesis was confirmed by a report that acute hepatitis in resolved HBV patients has a higher mortality rate than acute hepatitis in HBV-positive patients [23].

In addition, we found that the frequencies of HBV-specific $CD8^+$ T cells and $CD4^+Foxp3^+$ Tregs were reversible at the onset of HBV reactivation. These observations may imply that the reduction of $CD4^+Foxp3^+$ Tregs triggered the induction of antigen-specific CTLs. Although the effects of $CD4^+Foxp3^+$ Tregs are generally nonspecific or occur in a bystander manner, preferential inhibition of the antigen-specific T cell response has been observed in some cases, including human HBV infection [27]. In support of our results, Xu et al. [16] demonstrated that depletion of $CD4^+CD25^+$ Tregs led to an increase in HBV antigen-stimulated IFN-γ production and cellular proliferation of PBMCs in HBV-infected patients, and that coculture of $CD4^+CD25^+$ Tregs with effector cells significantly suppressed HBsAg-stimulated IFN-γ production and cellular proliferation. At the time of HBV reactivation in patient #6, when the number of $CD4^+Foxp3^+$ Tregs was increased, the reduction in serum HBV DNA was poor and liver damage was continuous. These findings suggest that a reduction in the number of $CD4^+Foxp3^+$ Tregs may induce an effective immune response.

We also observed that serum IL-7, IL-8 and MCP-1 were significantly higher in resolved HBV patients than in ICHB and CHB patients. However, the group of resolved HBV patients was quite miscellaneous and it remains unknown whether the differences among such cytokines and chemokines are responsible for HBV.

It has been demonstrated that IL-7 is required for T cell development and for maintaining and restoring the homeostasis of mature T cells. Administration of recombinant human IL-7 to patients resulted in widespread T cell proliferation, increased T cell numbers, modulation of peripheral T cell subsets and increased T cell receptor repertoire diversity [28]. Furthermore, IL-7 expression by hepatocytes directly controls T cell immune responses to Toll-like receptor signaling in vivo [29]. These observations suggest that IL-7 plays an important role for HBV-specific $CD8^+$ T cell proliferation and that a low level of IL-7 may be involved in the low frequencies of HBV-specific $CD8^+$ T cells in ICHB and CHB patients.

As previously reported, since rituximab therapy is a high risk factor for HBV reactivation, we examined a possible imbalance in serum Th1/Th2 cytokine secretion in HBV reactivation patients. As shown in supplementary Fig. 2, we analyzed the ratio of serum Th1/Th2 cytokines as follows: IFN-γ or IL-12 compared with IL-4 or IL-10. We observed a shift towards IL-10 compared with IFN-γ. However, when we compared IL-12 with IL-4 and IL-10, we observed a shift towards IL-12. Thus, we did not detect an obvious shift towards either Th1 or Th2 cytokines in the serum at the onset of HBV reactivation.

Finally, our study showed that HBV-specific $CD8^+$ T cells are increased at the onset of HBV reactivation despite an immunosuppressive status and declined following resolution of liver disease. In contrast, a reduced number of $CD4^+Foxp3^+$ Tregs was also observed and showed a negative correlation with the frequency of HBV-specific $CD8^+$ T cells. We plan to analyze additional resolved HBV patients prospectively and to clarify the relationships among $CD4^+Foxp3^+$ Tregs, HBV-specific $CD8^+$ T cells and liver damage.

Acknowledgments The authors thank Dr. Yasuhito Tanaka and Shigeru Kusumoto (Nagoya City University School of Medicine) for advice and experimental support. Supported by a grant from the Ministry of Education, Culture, Sports, Science and Technology of Japan and a grant-in-aid for specially promoted research on viral diseases from the Tokyo Metropolitan Government.

Conflict of interest The authors have no conflicts of interest to disclose.

References

1. Hoofnagle JH. Reactivation of hepatitis B. Hepatology. 2009;49:S156–65.
2. Raimondo G, Pollicino T, Cacciola I, Squadrito G. Occult hepatitis B virus infection. J Hepatol. 2007;46:160–70.
3. Yang JD, Roberts LR. Hepatocellular carcinoma: a global view. Nat Rev Gastroenterol Hepatol. 2010;7:448–58.
4. McMahon BJ. The natural history of chronic hepatitis B virus infection. Hepatology. 2009;49:S45–55.
5. Mason AL, Xu L, Guo L, Kuhns M, Perrillo RP. Molecular basis for persistent hepatitis B virus infection in the liver after clearance of serum hepatitis B surface antigen. Hepatology. 1998;27:1736–42.
6. Rehermann B, Ferrari C, Pasquinelli C, Chisari FV. The hepatitis B virus persists for decades after patients' recovery from acute viral hepatitis despite active maintenance of a cytotoxic T-lymphocyte response. Nat Med. 1996;2:1104–8.
7. Chisari FV, Ferrari C. Hepatitis B virus immunopathogenesis. Annu Rev Immunol. 1995;13:29–60.
8. Kimura K, Kakimi K, Wieland S, Guidotti LG, Chisari FV. Activated intrahepatic antigen-presenting cells inhibit hepatitis B virus replication in the liver of transgenic mice. J Immunol. 2002;169:5188–95.
9. Vento S, Cainelli F, Longhi MS. Reactivation of replication of hepatitis B and C viruses after immunosuppressive therapy: an unresolved issue. Lancet Oncol. 2002;3:333–40.
10. Sugauchi F, Tanaka Y, Kusumoto S, Matsuura K, Sugiyama M, Kurbanov F, et al. Virological and clinical characteristics on reactivation of occult hepatitis B in patients with hematological malignancy. J Med Virol. 2011;83:412–8.
11. Barber DL, Wherry EJ, Masopust D, Zhu B, Allison JP, Sharpe AH, et al. Restoring function in exhausted CD8 T cells during chronic viral infection. Nature. 2006;439:682–7.
12. Velu V, Kannanganat S, Ibegbu C, Chennareddi L, Villinger F, Freeman GJ, et al. Elevated expression levels of inhibitory receptor programmed death 1 on simian immunodeficiency virus-specific CD8 T cells during chronic infection but not after vaccination. J Virol. 2007;81:5819–28.
13. Zhang JY, Zhang Z, Wang X, Fu JL, Yao J, Jiao Y, et al. PD-1 up-regulation is correlated with HIV-specific memory CD8+ T-cell exhaustion in typical progressors but not in long-term nonprogressors. Blood. 2007;109:4671–8.
14. Urbani S, Amadei B, Tola D, Massari M, Schivazappa S, Missale G, et al. PD-1 expression in acute hepatitis C virus (HCV) infection is associated with HCV-specific CD8 exhaustion. J Virol. 2006;80:11398–403.
15. Kimura K, Ando K, Tomita E, Ohnishi H, Ishikawa T, Kakumu S, et al. Elevated intracellular IFN-gamma levels in circulating $CD8^+$ lymphocytes in patients with fulminant hepatitis. J Hepatol. 1999;31:579–83.
16. Xu D, Fu J, Jin L, Zhang H, Zhou C, Zou Z, et al. Circulating and liver resident $CD4^+$ $CD25^+$ regulatory T cells actively influence the antiviral immune response and disease progression in patients with hepatitis B. J Immunol. 2006;177:739–47.
17. Blackburn SD, Shin H, Haining WN, Zou T, Workman CJ, Polley A, et al. Coregulation of $CD8^+$ T cell exhaustion by multiple inhibitory receptors during chronic viral infection. Nat Immunol. 2009;10:29–37.
18. Wherry EJ, Ha SJ, Kaech SM, Haining WN, Sarkar S, Kalia V, et al. Molecular signature of $CD8^+$ T cell exhaustion during chronic viral infection. Immunity. 2007;27:670–84.
19. Guidotti LG, Rochford R, Chung J, Shapiro M, Purcell R, Chisari FV. Viral clearance without destruction of infected cells during acute HBV infection. Science. 1999;284:825–9.
20. Au WY, Lie AK, Liang R, Liu CL, Shek TW, Lau GK. Aggressive hepatocellular carcinoma complicating pregnancy after autologous bone marrow transplantation for non-Hodgkin's lymphoma. Bone Marrow Transplant. 2002;29:177–9.
21. Kojima H, Abei M, Takei N, Mukai Y, Hasegawa Y, Iijima T, et al. Fatal reactivation of hepatitis B virus following cytotoxic chemotherapy for acute myelogenous leukemia: fibrosing cholestatic hepatitis. Eur J Haematol. 2002;69:101–4.
22. Seth P, Alrajhi AA, Kagevi I, Chaudhary MA, Colcol E, Sahovic E, et al. Hepatitis B virus reactivation with clinical flare in allogeneic stem cell transplants with chronic graft-versus-host disease. Bone Marrow Transplant. 2002;30:189–94.
23. Kusumoto S, Tanaka Y, Ueda R, Mizokami M. Reactivation of hepatitis B virus following rituximab-plus-steroid combination chemotherapy. J Gastroenterol. 2011;46:9–16.
24. Liang R, Lau GK, Kwong YL. Chemotherapy and bone marrow transplantation for cancer patients who are also chronic hepatitis B carriers: a review of the problem. J Clin Oncol. 1999;17:394–8.
25. Araki K, Gangappa S, Dillehay DL, Rouse BT, Larsen CP, Ahmed R. Pathogenic virus-specific T cells cause disease during treatment with the calcineurin inhibitor FK506: implications for transplantation. J Exp Med. 2010;207:2355–67.
26. Wherry EJ. T cell exhaustion. Nat Immunol. 2011;12:492–9.
27. Alatrakchi N, Koziel M. Regulatory T cells and viral liver disease. J Viral Hepat. 2009;16:223–9.
28. Mackall CL, Fry TJ, Gress RE. Harnessing the biology of IL-7 for therapeutic application. Nat Rev Immunol. 2011;11:330–42.
29. Sawa Y, Arima Y, Ogura H, Kitabayashi C, Jiang JJ, Fukushima T, et al. Hepatic interleukin-7 expression regulates T cell responses. Immunity. 2009;30:447–57.

Biochimica et Biophysica Acta 1820 (2012) 1886–1892

Contents lists available at SciVerse ScienceDirect

Biochimica et Biophysica Acta

journal homepage: www.elsevier.com/locate/bbagen

Different mechanisms of hepatitis C virus RNA polymerase activation by cyclophilin A and B in vitro

Leiyun Weng [a], Xiao Tian [a], Yayi Gao [a], Koichi Watashi [b], Kunitada Shimotohno [c], Takaji Wakita [b], Michinori Kohara [d], Tetsuya Toyoda [a,d,e,*]

[a] Unit of Viral Genome Regulation, Institut Pasteur of Shanghai, Chinese Academy of Sciences, 411 Hefei Road, 200025 Shanghai, People's Republic of China
[b] Department of Virology II, National Institute of Health, 1-23-1 Toyama, Shinjuku, Tokyo 132-8640, Japan
[c] Chiba Institute of Technology, 2-17-1 Tsudamuna, Narashino, Chiba 275-0016, Japan
[d] Department of Microbiology and Cell Biology, The Tokyo Metropolitan Institute of Medical Science, 2-1-6 Kamikitazawa, Setagaya-Ku, Tokyo 156-8506, Japan
[e] Choju Medical Institute, Fukushimura Hospital, 19-14 Azanakayama, Noyori-cho, Toyohashi, Aichi 441-8124, Japan

ARTICLE INFO

Article history:
Received 26 April 2012
Received in revised form 25 July 2012
Accepted 21 August 2012
Available online 28 August 2012

Keywords:
HCV
RNA polymerase
Cyclophilin A
Cyclophilin B

ABSTRACT

Background: Cyclophilins (CyPs) are cellular proteins that are essential to hepatitis C virus (HCV) replication. Since cyclosporine A was discovered to inhibit HCV infection, the CyP pathway contributing to HCV replication is a potential attractive stratagem for controlling HCV infection. Among them, CyPA is accepted to interact with HCV nonstructural protein (NS) 5A, although interaction of CyPB and NS5B, an RNA-dependent RNA polymerase (RdRp), was proposed first.
Methods: CyPA, CyPB, and HCV RdRp were expressed in bacteria and purified using combination column chromatography. HCV RdRp activity was analyzed in vitro with purified CyPA and CyPB.
Results: CyPA at a high concentration (50× higher than that of RdRp) but not at low concentration activated HCV RdRp. CyPB had an allosteric effect on genotype 1b RdRp activation. CyPB showed genotype specificity and activated genotype 1b and J6CF (2a) RdRps but not genotype 1a or JFH1 (2a) RdRps. CyPA activated RdRps of genotypes 1a, 1b, and 2a. CyPB may also support HCV genotype 1b replication within the infected cells, although its knockdown effect on HCV 1b replicon activity was controversial in earlier reports.
Conclusions: CyPA activated HCV RdRp at the early stages of transcription, including template RNA binding. CyPB also activated genotype 1b RdRp. However, their activation mechanisms are different.
General significance: These data suggest that both CyPA and CyPB are excellent targets for the treatment of HCV 1b, which shows the greatest resistance to interferon and ribavirin combination therapy.

1. Introduction

Hepatitis C virus (HCV[1]), which belongs to the *Flaviviridae* family, has a positive-strand RNA genome, and its replication is regulated by viral and cellular proteins [1]. The genome encodes a large precursor polyprotein that is cleaved by host and viral proteases to generate at least 10 functional viral proteins: core, envelope 1 (E1), E2, p7, nonstructural protein 2 (NS2), NS3, NS4A, NS4B, NS5A, and NS5B [2]. NS5B is an RNA-dependent RNA polymerase (RdRp) [3–5].

HCV frequently establishes a persistent infection that leads to chronic hepatitis, liver cirrhosis, and hepatocellular carcinoma [6,7]. More than 170 million individuals worldwide are infected with HCV [8], and the challenge of developing HCV treatment continues. First, combination therapy with pegylated interferon α (Peg-IFNα) and ribavirin led to a sustained virological response (SVR) in approximately 55% of patients infected with any HCV genotype and 42–46% of patients with genotype 1 [9,10]. However, many patients could not tolerate the serious adverse effects. Triple therapy consisting of an NS3/NS4A protease inhibitor (boceprevir or telaprevir), Peg-IFN (α-2a or α-2b), and ribavirin was then introduced, and it has become the standard regimen for genotype 1 infection. SVR improved significantly (from 63% to 75%), and the treatment duration decreased from 12 to 6 months [11,12]. However, triple therapy is more toxic than combination therapy [13].

Nonimmunosuppressant cyclosporine A (CsA) analogues/CyP inhibitors such as DEBIO-025 (Alisporivir) [14], NIM811 [15], and SCY-635 [16] are also the most expected candidates for use as anti-HCV drugs because their resistance selection is rare compared with other direct-acting antiviral agents, and the HCV resistant to

Abbreviations: BSA, bovine serum albumin; CsA, cyclosporine A; CyP, cyclophilin; DTT, dithiothreitol; E, envelope; EDTA, ethylenediaminetetraacetic acid; GST, glutathione S-transferase; HCV, hepatitis C virus; NS, nonstructural protein; PPI, peptidyl prolyl *cis/trans*-isomerases; Peg-IFN, pegylated interferon-α; PMSF, phenylmethanesulfonylfluoride; RT-PCR, reverse transcription polymerase chain reaction; RdRp, RNA-dependent RNA polymerase; SDS-PAGE, sodium dodecyl sulfate polyacrylamide gel electrophoresis analysis; SVR, sustained virological response; ΔPPI, PPI knockout; wt, wild type

* Corresponding author at: Choju Medical Institute, Fukushimura Hospital, 19-4 Azanakayama, Noyori-cho, Toyohashi, Aichi 441-8124, Japan. Tel.: +81 532 46 7511; fax: +81 532 46 8940.
E-mail address: toyoda_tetsuya@yahoo.co.jp (T. Toyoda).

0304-4165/$ – see front matter © 2012 Elsevier B.V. All rights reserved.
http://dx.doi.org/10.1016/j.bbagen.2012.08.017

CyP inhibitors acquired mutations that allowed for reduced dependence on CyPs [17,18].

CyP was originally discovered as a cellular factor with high affinity for CsA [19]. CyPs comprise a family of peptidyl prolyl *cis/trans*-isomerases (PPI) that catalyze the *cis–trans* interconversion of peptide bonds amino terminal to proline residues, facilitating protein conformation changes [20]. CyPs are potential antiviral targets because CyPA was found to play a critical role in human immunodeficiency virus-1 infection [21,22]. The role of human CyPs as cellular cofactors in HCV replication was first suggested upon discovery of the anti-HCV effect of CsA [23–26]. Although the completion of a binding assay and the mapping of resistance initially suggested that NS5B was a viral target for CsA [27–29], recent papers have pointed to CyPA and NS5A as the central virus–host interaction involved in HCV replication [30–36]. Despite this unfavorable evidence, we analyzed the effect of CyPA and CyPB on HCV RdRp of various genotypes in vitro and found differences in genotype specificity and the mechanism of HCV RdRp activation.

2. Materials and methods

2.1. Purification of HCV RdRp

HCV RNA RdRps with C-terminal 21 amino acid deletion of 1a (H77 and RMT), 1b (HCR6, NN, and Con1), and 2a (JFH1 and J6CF) were expressed in *E. coli* Rosetta/pLysS and purified as described previously [37–40]. The purified HCV RdRps (5 μM, >95% pure) were stocked in 20 mM Tris–HCl (pH 8.0), 500 mM NaCl, 1 mM ethylenediaminetetraacetic acid (EDTA), 5 mM dithiothreitol (DTT), 5% glycerol, and 1 mM phenylmethanesulfonylfluoride (PMSF) at −80 °C. The yield of HCV RdRps is approximately 1.7 mg from a 1-L bacterial culture. The purified HCV RdRps were as shown in Fig. S1 of Weng et al. [38]. The protein purities were determined by sodium dodecyl sulfate polyacrylamide gel electrophoresis analysis (SDS-PAGE), using ImageJ 1.46 (http://rsbweb.nih.gov/ij/).

2.2. Construction of CyP-expressing plasmids

Human CyPA and CyPB were cloned from total RNA extracted from 293T cells, using a reverse transcription-polymerase chain reaction (RT-PCR) kit (Takara, Dalian, China) as published previously [29]. After being digested with *Bam*HI and *Eco*RI, they were cloned into the same site of pGEX-6P-3 (GE Healthcare, Bucks, UK), resulting in pGEXCyPA and pGEXCyPB, respectively. CyPBΔPPI, the enzymatic inactive mutant of CyPB, was PCR cloned into pGEX-6P-3 from pCMV-CyPBΔPPIFL [29], resulting in pGEXCyPBΔPPI. CyPAΔPPI was produced by the introduction of the R55A and F60A mutations using a QuickChangeII Site-Directed Mutagenesis Kit (Stratagene, St. Clara, CA, USA) and primers (5′-GTTCCTGCTTTCACGCCATTATTCCAGGGG CCATGTGTCAGGGTG-3′ and 5′-CACCCTGACACATGGCCCCTGGAATAA TGGCGTGAAAGCAGGAAC-3′).

2.3. Purification of CyPs

E. coli Rosetta were transformed using pGEXCyPA, pGEXCyPAΔPPI, pGEXCyPB, and pGEXCyPBΔPPI. GST-tagged CyPA, CyPB, CyPAΔPPI, and CyPBΔPPI were induced with 1 mM isopropyl β-D-1-thiogalactopyranoside at 18 °C for 4 h. The bacteria were harvested and stocked at −20 °C. After thawing on ice, the bacteria were lysed in 4 packed cell volumes of phosphate-buffered saline, 0.1% Triton X-100, 1 mM EDTA, 1 mM DTT, and 1 mM PMSF. After being clarified by centrifugation at 10,000×*g* for 30 min at 4 °C and filtered through a 0.45-μm nitrocellulose filter, the extract was incubated with Glutathione Sepharose 4B (GE Healthcare) for 30 min at 4 °C. After the resin was washed with 50 mM Tris–HCl (pH 8.0), 500 mM NaCl, 1 mM EDTA, 1 mM DTT, and 1 mM PMSF, the GST-CyP was eluted using 50 mM Tris–HCl (pH 8.0), 500 mM NaCl, 1 mM EDTA, 1 mM DTT, 10 mM reduced glutathione, and 1 mM PMSF, followed by gel filtration through a Superdex 200 column (GE Healthcare) in 20 mM Tris–HCl (pH 8.0), 500 mM NaCl, 1 mM EDTA, 1 mM DTT, and 10% glycerol. The eluted GST-CyP were diluted to 50 mM NaCl and applied to a MonoQ (GE Healthcare) in 20 mM Tris–HCl (pH 9.0), 50 mM NaCl, 1 mM EDTA, 1 mM DTT, and 10% glycerol. GST-CyPB and GST-CyPBΔPPI were chromatographed using a continuous NaCl gradient of 50–1000 mM. The purified CyPs were stocked at −20 °C.

2.4. In vitro HCV transcription with CyPs

In vitro HCV transcription with CyPs was done as previously described [37–40]. Briefly, the indicated amounts of the CyPs were incubated in 50 mM Tris–HCl (pH 7.5), 200 mM monopotassium glutamate, 3.5 mM $MnCl_2$, 1 mM DTT, 0.5 mM GTP, 200 nM of a 184-nt in vitro transcribed model RNA template (SL12-1S), 100 U/mL of human placental RNase inhibitor, and 100 nM HCV RdRp at 29 °C for 30 min. After preincubation, RdRp was incubated for an additional 90 min with 50 μM ATP, 50 μM CTP, or 5 μM [α-^{32}P]UTP. The RNA products were analyzed using 6% PAGE containing 8 M urea after being purified by phenol/chloroform extraction and ethanol precipitation. The amount of RNA products was analyzed using Typhoon Trio (GE Healthcare).

2.5. RNA filter-binding assay with CyPA and CyPB

An RNA filter-binding assay with CyPA and CyPB was performed as previously described [37,38,40]. Briefly, [^{32}P]-SL12-1S was incubated in 25 μL of 50 mM Tris–HCl (pH 7.5), 200 mM monopotassium glutamate, 3.5 mM $MnCl_2$, 1 mM DTT, and 5 pmol of HCV RdRp with 375 pmol (75×) of CyPA and 25 pmol (5×) of CyPB at 29 °C for 30 min.

2.6. Chemicals and radioisotopes

[α-^{32}P]UTP (800 Ci/mmol, 40 mCi/mL) was purchased from PerkinElmer Life Sciences (Waltham, MA, USA). The nucleotides were purchased from GE Healthcare. The human placental RNase inhibitor T7 RNA polymerase and PrimeSTAR HS DNA polymerase were purchased from Takara. The bacteria were purchased from Novagen (Merck Chemicals, Darmstadt, Germany).

2.7. Statistical analysis

The statistical data were evaluated using Student's *t* test, with $p<0.05$ indicating statistical significance.

3. Results

3.1. Purification of CyPA and B

First, glutathione S-transferase (GST)-tagged CyPA, CyPB, the PPI inactive CyPA (CyPAΔPPI), and CyPB (CyPBΔPPI) were purified using Glutathione Sepharose 4B affinity chromatography. CyPA and CyPAΔPPI were further purified through a Superdex 200 column (Fig. S1). After the Superdex 200 gel filtration, to remove the contaminating nucleic acids, CyPB and CyPBΔPPI were further purified through MonoQ anion exchange chromatography by a continuous NaCl gradient of 50–1000 mM because CyPB has a strong affinity for nucleic acids. Each was eluted with 210–385 mM NaCl (Fig. S2). The purification scheme and purified CyPs are shown in Fig. 1. The yields of CyPA and CyPAΔPPI were approximately 3 mg from a 1-L bacterial culture. CyPA and CyPAΔPPI were >95% pure and stocked at 5 mg/mL in 20 mM Tris–HCl (pH 8.0), 500 mM NaCl, 1 mM EDTA, 1 mM DTT, and 10% glycerol. CyPB and CyPBΔPPI were stocked at 5 mg/mL in 20 mM Tris–HCl (pH 9.0), 500 mM NaCl, 1 mM EDTA, 1 mM DTT,

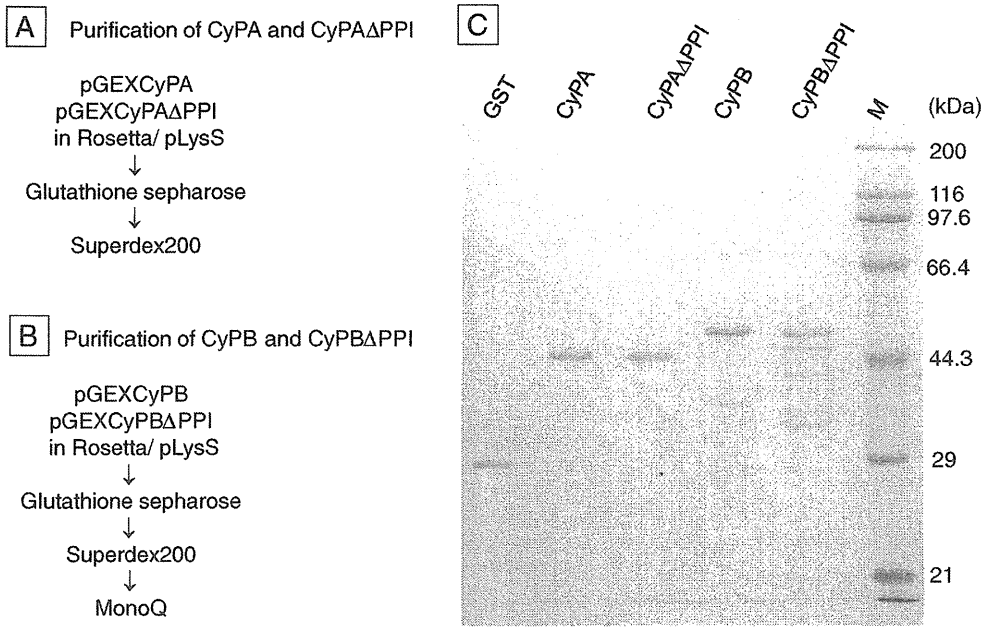

Fig. 1. Cyclophilin purification. The purification schemes of cyclophilin A (CyPA) and the peptidyl prolyl isomerase-inactive mutant protein of CyPA (CyPAΔPPI) (A), cyclophilin B (CyPB) and CyPBΔPPI (B), and sodium dodecyl sulfate-polyacrylamide gel electrophoresis (SDS-PAGE) (C) with 5 pmol each of purified glutathione S-transferase (GST; 28.3 kDa), GST-CyPA (44.9 kDa), GST-CyPAΔPPI (44.7 kDa), GST-CyPB (52.1 kDa), and GST-CyPBΔPPI (52 kDa) were separated through 10% SDS-PAGE and stained with Coomassie brilliant blue. The sizes of the molecular weight standards (M) are indicated on the right side of the gel. Their final elution profiles are shown in Figs. S1 and S2.

and 10% glycerol. The yields of CyPB and CyPBΔPPI were approximately 1 mg from a 1-L bacterial culture. The purities of CyPB and CyPBΔPPI were >95% and >90%, respectively.

3.2. HCV 1b and JFH1 (2a) transcription in vitro with CyPA and CyPB

The dose–response effects of CyPA and CyPB were examined using an in vitro transcription system of HCR6 (1b) and JFH1 (2a) RdRp wild type (wt). CyPA and CyPB were added to the optimal HCV in vitro transcription condition while the RNA synthesis was in the log phase [4,37]. RdRp (100 nM) was incubated with 0, 50 (ratio to RdRp: 0.5×), 100 (1×), 200 (2×), 500 (5×), and 1000 nM (10×) CyPA and CyPB, GST, or bovine serum albumin (BSA) in GTP (the initiating nucleotide) and an RNA template for 30 min, followed by elongation with ATP, CTP, and UTP for 90 min. CyPA enhancement was further tested using 2 (20×), 5 (50×), 7.5 (75×), and 10 (100×) μM because the enhancement effect of CyPA under 1 μM (10×) was unclear. Fig. S3 shows the autoradiography of HCV HCR6 (1b) and JFH1 (2a) RdRpwt with CyPA and CyPB, the graphs of which were drawn using the data from 3 independent experiments (Fig. 2).

The CyPA activation of both RdRps showed 2 reaction speeds. The first-order ratio of CyPA to HCR6 (1b) RdRpwt<50× is fitted as a linear regression curve, the equation for which is $y = 0.07x$ (CyPA-to-RdRp ratio) + 0.7. The linear regression curve fitting of the ratio >50× is $y = 0.4x$ (CyPA-to-RdRp ratio) − 17 when calculated from 3 points. That of CyPA to JFH1 (2a) RdRpwt is fitted to a similar linear regression, $y = 0.09x$ (CyPA-to-RdRp ratio) + 0.9 (the CyPA-to-RdRp ratio<50×). HCVR6 (1b) and JFH1 (2a) RdRps were activated by 100× CyPA to 25-±0.2- and 19-±1-fold, respectively.

The CyPB activation of HCR6 (1b) RdRpwt occurred in a dose-dependent manner and fitted a sigmoid curve, and the enhancement effect reached a plateau (9.4×) at the ratio of 5×. Neither GST nor BSA enhanced HCR6 (1b) RdRpwt. CyPB, GST, and BSA did not enhance JFH1 (2a) RdRpwt (<1.5×) at the concentrations described earlier.

3.3. Effect of the PPI inactive mutant proteins of CyPA and CyPB

CyP has PPI activity. To test the contribution of PPI activity to HCV HCR6 (1b) and JFH1 (2a) RdRpwt activation, the activation effect of the PPI inactive mutant proteins, CyPAΔPPI at 100× (10 μM) and CyPBΔPPI at 2× (200 nM), were tested together with 100× (10 μM) GST and BSA (Fig. 3). CyPA enhanced JFH1 (2a) RdRpwt 17.6×, whereas CyPAΔPPI enhanced it 16.2×. This difference is statistically significant (Student's t test, $p<0.05$). CyPA enhanced HCR6 (1b) RdRpwt activity 27.7×, whereas CyPAΔPPI enhanced it 16.0×. BSA slightly inhibited both RdRps at the same concentration in this experiment. As shown in Fig. 2C and D, it can be concluded that BSA has no effect on HCV transcription. GST enhanced JFH1 (2a) RdRpwt activity 5.0×, but it did not affect HCR6 (1b) RdRpwt activity. CyPB enhanced HCR6 (1b) RdRpwt activity 2.3×, whereas CyPBΔPPI enhanced it 1.7×. This difference is also statistically significant (Student's t test, $p<0.05$). JFH1 (2a) RdRpwt was not activated by CyPB or CyPBΔPPI.

3.4. CyP activation steps of HCV transcription

The HCV transcription steps of CyP enhancement were analyzed by the sequential addition of CyPs during in vitro transcription (Fig. 4). CyPA enhanced HCR6 (1b) and JFH1 (2a) RdRpwt, whereas CyPB enhanced HCR6 (1b) RdRpwt when HCV RdRps were incubated with them from the start of transcription (initiation). The CyP effect was then tested after their addition during the elongation period after HCV RdRps was initiated with GTP. CyPA (100×; 10 μM) and CyPB (5×; 500 nM) were added to HCV RdRps after the 30-min incubation with GTP, when 3 GTPs were incorporated at the 5′ end of the products. CyPB did not enhance HCR6 (1b) or JFH1 (2a) RdRp when added during the elongation period, although it enhanced HCV RdRp when added at the start of transcription. CyPA enhanced HCR6 (1b) and JFH1 (2a) RdRp activity only 1.6× (Student's t test, $p<0.05$) and 2.1× ($p<0.01$), respectively, when added during the elongation step. These results suggest that CyPA and CyPB activated only the transcription initiation step of HCV RdRps.

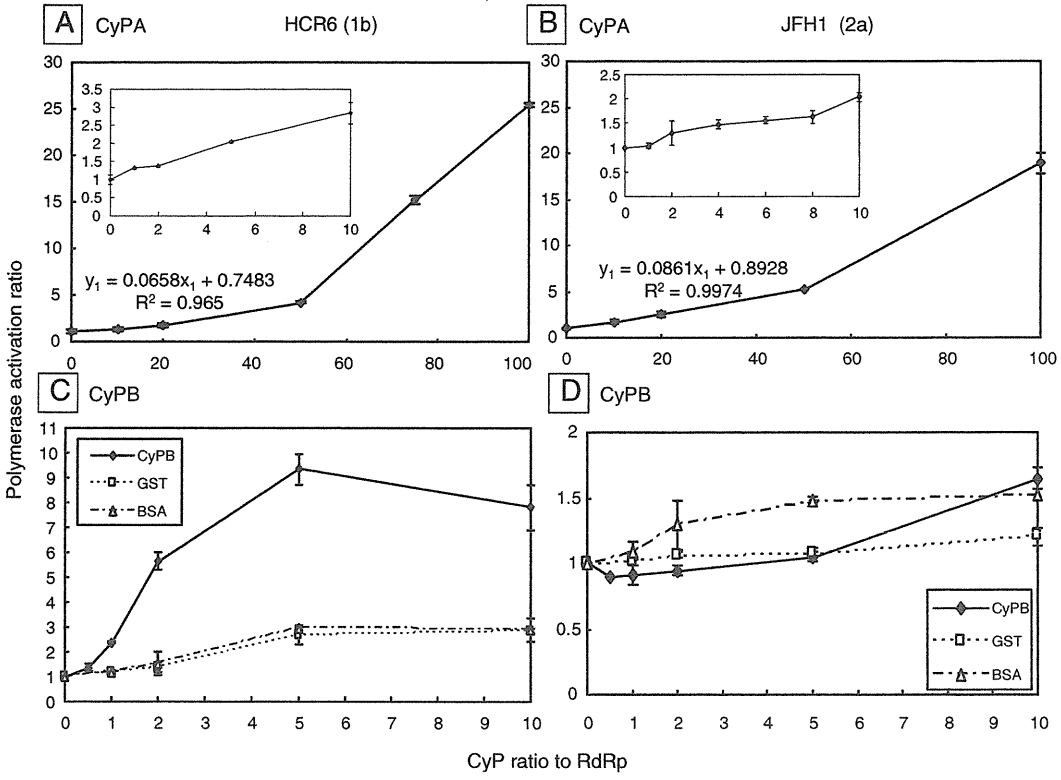

Fig. 2. Dose–response curve of cyclophilin A (CyPA) and cyclophilin B (CyPB) in hepatitis C virus (HCV) transcription in vitro. The dose–response curve of the HCV RdRp activation of CyPA in HCR6 (1b) RdRpwt (A) and JFH1 (2a) RdRpwt (B) CyPB in HCR6 (1b) RdRpwt (C) and JFH1 (2a) RdRpwt was drawn from the image analysis of Fig. S3. Insets A and B indicate that of 0, 0.5×, 1×, 2×, 5×, and 10× of CyPA to RdRp. The first-order ratio of the curves of A and B were fit by linear regression, and the calculated equations are indicated in the graph. The mean relative polymerase activation ratio and standard deviation (error bar) were calculated from 3 independent measurements.

The effects of 75× CyPA and 5× CyPB on the RNA-binding activity of HCR6 (1b) and JFH1 (2a) RdRp were then tested (Fig. 4E). The effects of HCR6 (1b) and JFH1 (2a) RdRp with CyPA were 10.1-±0.56- and 6.6-±0.68-fold of that without CyPA, respectively. The effect of HCR6 (1b) RdRp with CyPB was 3.1-±0.3-fold of that without CyPB. The RNA-binding activity of HCV RdRps was thus enhanced by the addition of CyPA and CyPB.

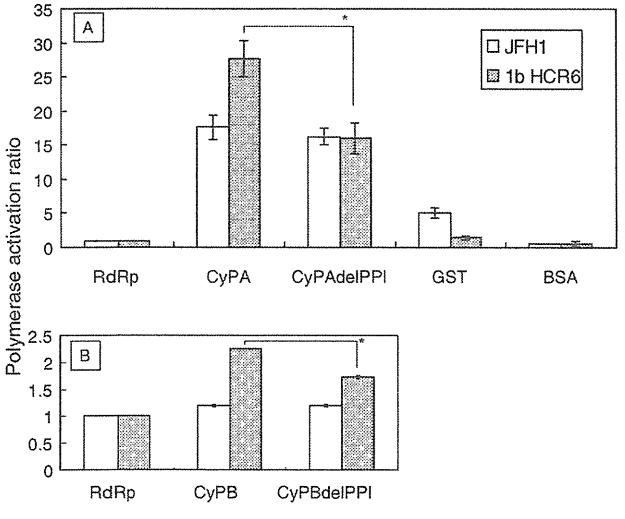

Fig. 3. Effects of cyclophilin A (CyPA) and cyclophilin B (CyPB) with and without peptidyl prolyl isomerases activity on hepatitis C virus (HCV) JFH1 (2a) and HCR6 (1b) RdRp. HCV HCR6 (1b) and JFH1 (2a) RdRpwt (100 nM) were incubated with 100× (10 μM) of CyPA, CyPAΔPPI, glutathione S-transferase (GST), and bovine serum albumin (BSA) (A). HCV RdRps were incubated with 5× (500 nM) of CyPB, CyPBΔPPI, GST, and BSA (B). The mean relative polymerase activity and standard deviation (error bar) were calculated from 3 independent measurements. *$p<0.01$ (Student's t test).

3.5. Effect of CyP activation on RdRp of various HCV genotypes

The CsA sensitivity differed among the HCV genotypes [41]. Therefore, we tested the effects of CyPA and CyPB activation on NN (1b), H77 (1a), RMT (1a), and J6CF (2a) RdRp (Fig. 5). RdRp activity was compared with and without 50× (5 μM) CyPA and 5× (500 nM) CyPB. At their respective concentrations, CyPA activated all of the tested HCV RdRps by 3.9–5.3×, but CyPB activated only 1b RdRps (8–10×). CyPB slightly activated J6CF (2a) RdRp (approximately 4×), but it did not activate the 1a or JFH1 (2a) RdRps (1.4–1.8×).

4. Discussion

Since CsA was discovered to inhibit HCV infection [23–26], the CyP pathway contributing to HCV replication has been proposed as a potential stratagem for controlling HCV infection. Reports about the roles of CyPA in HCV replication via NS5A have been accumulating [33–35,42–44]. However, the effect of CyP inhibitors varied on the RNA-binding activity of NS5B [41,45], and DEBIO-025 decreased CyPB levels in patients [46]. Controversial results of CyPA and CyPB knockout experiments on HCV replicon activity were reported [29,30,47]. Therefore, the effects of CyPA and CyPB on HCV RdRp were carefully analyzed again in vitro.

In this study, we demonstrated that CyPA and CyPB activated HCV 1b RdRp in vitro by completely different kinetics using purified CyPs